ELSEVIER

Coordination Chemistry Reviews 230 (2002) 107–125

COORDINATION CHEMISTRY REVIEWS

www.elsevier.com/locate/ccr

Electrochemistry of different types of photoreactive ruthenium(II) dicarbonyl α-diimine complexes

František Hartl *, Maxim P. Aarnts, Heleen A. Nieuwenhuis, Joris van Slageren

Institute of Molecular Chemistry, Universiteit van Amsterdam, Nieuwe Achtergracht 166, 1018 WV Amsterdam, The Netherlands

Received 25 January 2002; accepted 26 February 2002

Contents

Abstract

The photochemical reactivity, photophysical properties and redox behavior of the complexes *trans*,*cis*-[Ru(X)(X′)(CO)$_2$(α-diimine)] and their derivatives are strongly dependent on the complex geometry, the nature and electronic properties of the α-diimine ligand and, most importantly, on the axial ligands X and X′ (alkyl, halide, phosphine, donor solvent, etc.). This paper deals mainly with comparison of reduction pathways for several different types of the *trans*,*cis*-[Ru(X)(X′)(CO)$_2$(α-diimine)] complexes, also presenting some new results in this field. An equally important goal has been the comparison and discussion of the photo- and redox reactivity of these complexes from the viewpoint of the frontier orbitals involved and character of the Ru–X/X′ bonding.

Keywords: Diimine; Carbonyl; Ruthenium complexes; Photochemistry; Cyclic voltammetry; Spectroelectrochemistry; MLCT states; XLCT states; SBLCT states; Radicals; Anions; Reduction pathway; Bond cleavage

1. Introduction

Potential applications of photoinduced energy and electron transfer reactions as key processes in novel molecular photonic materials and devices have led to a large number of studies of the complexes [Ru(α-diimine)$_3$]$^{2+}$ [1–10]], *fac*-[Re(X)(CO)$_3$(α-diimine)]^n ($n = 0$ for X = halide; $n = +1$ for X = N-donor ligand, PR$_3$) [11–19] and polynuclear supramolecular systems composed of these building blocks connected by purpose-made bridging ligands [10,20–23]. The lowest excited state of most of these complexes can be assigned as metal-to-ligand charge transfer (MLCT). Both types of compounds show emission, the CT excited states of

* Corresponding author. Tel.: +31-20-525-6450; fax: +31-20-525-6456

E-mail address: hartl@science.uva.nl (F. Hartl).

0010-8545/02/$ - see front matter
PII: S0010-8545(02)00079-6

the Ru(II) complexes being somewhat more labile compared to those of the Re(I) complexes due to a transition to a thermally accessible dissociative ligand-field (LF) state [2,6,24]. Excitation into a low-energy MLCT transition is closely related to ligand-localized reduction of the same complex. This is confirmed by the fact that a number of photochemically initiated reactions also occur upon one-electron reduction or oxidation of the complex [25]. A well known example is the photo- or electrocatalyzed reduction of CO_2 to CO using the complexes *fac*-[Re(Cl)(CO)$_3$(bpy)] (bpy = 2,2-bipyridine) (in the presence of an electron donor such as triethanolamine or triethylamine) [26–31] or [Ru(X)$_{2-x}$(CO)$_x$(bpy)$_2$] (X = Cl, $x = 1, 2$) [32–34] as catalyst precursors. Other typical examples are the photochemical CO substitution reactions of [Cr(CO)$_4$(bpy)] with PPh_3 and of [Os(Cl)$_2$(CO)$_2$(bpy)] with acetonitrile, that also occur upon electrochemical reduction and oxidation, respectively [35–38].

In the case of the Re(I) complexes *fac*-[Re(X)(CO)$_3$(α-diimine)]^n ($n = 0, +1$), the properties and lifetime of the lowest excited state can be dramatically influenced by variation of the axial ligand X. For example, proceeding from X = Cl to I changes this excited state from MLCT to XLCT, while complexes with X = $SnPh_3$ or alkyl have a mixed SBLCT/MLCT (or $\sigma\pi^*/d_\pi\pi^*$) lowest excited state (SB stands for σ(Re–X) bond) [39]. Understanding this ligand dependence is of much interest, providing an opportunity to tune deliberately the photochemical reactivity and photophysical properties (e.g. luminescence) of the complexes.

Electrochemical studies of *fac*-[Re(X)(CO)$_3$(α-diimine)]^n have demonstrated that their reduction paths depend strongly on the π-acceptor capacity of the α-diimine ligand, i.e. on the energy of the predominantly π*(α-diimine) LUMO of the complexes [40–42]. Nevertheless, the influence of the strength of the Re–X bond in the reduced complexes is also significant. Thus, for complexes with X = halide the stability of the primarily formed one-electron-reduced radical anions *fac*-[Re(X)(CO)$_3$(α-diimine)]$^{\bullet -}$ was found to be rather limited for the complexes with relatively high-lying π*(α-diimine) levels. Their generation is accompanied by facile dissociation of X, with the rate increasing in the order Cl ≪ Br < I, and formation of five-coordinate radicals [Re(CO)$_3$(α-diimine)]$^\bullet$. The latter reactive species either dimerize to [Re(CO)$_3$(α-diimine)]$_2$ or become stabilized by coordination of a donor solvent (Sv) or PR_3 (Eqs. (1)–(4)) [40,41]. The electronic properties of the reduced α-diimine ligand and the axial ligands X also determine the structure of the products of the second one-electron reduction step, that are either the five-coordinate anions [Re(CO)$_3$(α-diimine)]$^-$ with a delocalized Re(α-diimine) π-bonding, or the six-coordinate anions *fac*-[Re(X)(CO)$_3$(α-diimine)]$^-$ (X = e.g. CH_3CN or $P(OR)_3$) in which both added electrons largely occupy the lowest π*(α-diimine) orbital (Eqs. (5)–(7)) [31,40,43]. For α-diimine = 2,2′-bipyridine (bpy), both five-coordinate reduction products, the one-electron reduced radical [Re(CO)$_3$(bpy)]$^\bullet$ and the two-electron reduced anion [Re(CO)$_3$(bpy)]$^-$, have been proposed to be the active species in the electrocatalyzed reduction of CO_2 [44]. A comprehensive IR spectroelectrochemical investigation of these systems has recently provided a direct evidence for the validity of this proposal and contributed significantly to the description of the complex catalytic mechanisms [31]. In contrast to the photostable and irreversibly reducible complexes *fac*-[Re(X)(CO)$_3$(α-diimine)] with X = halide, their photoreactive analogues with X = alkyl are reduced to fairly stable radical anions even for rather basic α-diimine ligands such as 2,2′-bipyridine or for non-aromatic α-diimine ligands such as *N*,*N*′-dialkyl-1,4-diaza-1,3-butadienes (R-DAB) [45,46]. Apparently, the strength of the Re–alkyl bond in the dissociative ^{3}SBLCT/MLCT (or $^3\sigma\pi^*/d_\pi\pi^*$) excited state is considerably more affected by removal of the electron from the predominantly σ(Re–alkyl) HOMO than by the occupation of the predominantly π*(α-diimine) LUMO.

$$fac\text{-[Re(X)(CO)}_3(\alpha\text{-diimine)]} + e^- \rightarrow (fac\text{-[Re(X)(CO)}_3(\alpha\text{-diimine)]}^{\bullet -} \quad (1)$$

$$fac\text{-[Re(X)(CO)}_3(\alpha\text{-diimine)]}^{\bullet -} \rightarrow [Re(CO)_3(\alpha\text{-diimine)}]^\bullet + X^- \quad (2)$$

$$[Re(CO)_3(\alpha\text{-diimine)}]^\bullet \rightarrow [Re(CO)_3(\alpha\text{-diimine)}]_2 \quad (3)$$

$$[Re(CO)_3(\alpha\text{-diimine)}]^\bullet + Sv \rightarrow fac\text{-[Re(Sv)(CO)}_3(\alpha\text{-diimine)}]^\bullet \quad (4)$$

$$[Re(CO)_3(\alpha\text{-diimine)}]_2 + 2e^- \rightarrow 2\,[Re(CO)_3(\alpha\text{-diimine)}]^- \quad (5)$$

$$fac\text{-[Re(Sv)(CO)}_3(\alpha\text{-diimine)}]^\bullet + e^- \rightarrow fac\text{-[Re(Sv)(CO)}_3(\alpha\text{-diimine)}]^- \quad (6)$$

$$fac\text{-[Re(Sv)(CO)}_3(\alpha\text{-diimine)}]^- \Leftrightarrow [Re(CO)_3(\alpha\text{-diimine)}]^- + Sv \quad (7)$$

Related complexes *fac*-[Mn(X)(CO)$_3$(α-diimine)] (X = halide, alkyl) have also been recently studied by combined (spectro)electrochemical techniques at variable temperatures [47]. Compared with their Re analogues, the singly reduced radical complexes [Mn(CO)$_3$(α-diimine)]$^\bullet$ have an increased tendency to dimerize, while the doubly reduced species preferably exist as stable, relatively unreactive five-coordinate anions [Mn(CO)$_3$(α-diimine)]$^-$. This behavior reflects the significantly increased metal character of the highest occupied orbitals in the reduced complexes, as was also concluded from the resonance Raman spectrum of the anion [Mn(CO)$_3$(*i*Pr-DAB)]$^-$ and DFT MO calculations [48,49]. The detailed knowledge of the reduction pathways of the complexes *fac*-[Mn(X)(CO)$_3$(α-diimine)] (X = halide, α-diimine = bpy, *i*Pr-DAB) has been of a crucial importance for understanding their intriguing

MLCT/XLCT photoreactivity in coordinating solvents (Sv) at low temperatures [50]. Under these conditions illumination of the *fac*-[Mn(X)(CO)$_3$(α-diimine)] complexes ultimately produces the two-electron reduced anions [Mn(CO)$_3$(α-diimine)]$^-$ via a radical-disproportionation reaction between [Mn(CO)$_3$(α-diimine)]$^\bullet$ and *fac*-[Mn(Sv)(CO)$_3$(α-diimine)]$^\bullet$ (Scheme 1). On the grounds of the spectro-electrochemical studies it has also been proposed that the dimer [Mn(CO)$_3$(α-diimine)]$_2$, formed as the ultimate photoproduct at ambient temperatures, not only arises from the direct dimerization of [Mn(CO)$_3$(α-diimine)]$^\bullet$, but at least partly also from a coupling reaction between the photochemically generated anions [Mn(CO)$_3$(α-diimine)]$^-$ and parent complex *fac*-[Mn(X)(CO)$_3$(α-diimine)] (Scheme 1) [47].

Similarly to analogous rhenium complexes, *fac*-[Mn(X)(CO)$_3$(α-diimine)] (X = alkyl) also produce alkyl radicals by efficient homolytic splitting of the Mn–alkyl bond from the lowest-energy excited states of mixed ^{3}SBLCT/MLCT character [51]. In particular the complex *fac*-[Mn(Bz)(CO)$_3$(*i*Pr-DAB)] (Bz = benzyl) has been found to be a very promising visible-light photoinitiator of free radical polymerization [52]. In this case crossing from the lowest optically accessible MLCT to the reactive ^{3}SBLCT state at a lower energy occurs with high quantum efficiency. On the other hand, a CO loss photoreaction was observed for *fac*-[Mn(Me)(CO)$_3$(*i*Pr-DAB)] from its reactive lowest-energy excited state of a prevailing ^{3}MLCT character [51]. In contrast to this pronounced alkyl-dependent photochemical reactivity, the electrochemically produced radical anions *fac*-[Mn(X)(CO)$_3$(α-diimine)]$^{\bullet -}$ are stable enough to be detected by cyclic voltammetry (CV) at moderate scan rates [47]. Their stability is much higher compared to analogous radical anions with halide ligands, but cannot compete with the stable one-electron reduced alkylrhenium complexes [45,46].

The opportunity to vary two non-carbonyl co-ligands in the Mn and Re α-diimine complexes has been so far limited to *trans*(X)-[M(X)$_2$(CO)$_2$(α-diimine)]$^+$ (M = Mn, Re, X = PR$_3$, P(OR)$_3$; M = Mn, X = CNBu^t) and *trans*,*cis*-[Mn(COMe)(CNBu^t)(CO)$_2$(α-diimine)] [47,53–55]. From this viewpoint d^6 Ru(II) complexes *trans*,*cis*-[Ru(X)(X′)(CO)$_2$(α-diimine)] and their *cis*,*cis*-isomers represent a very useful class of coordination compounds, where the simultaneous variation of different types of X and X′ co-ligands is facile and offers fascinating opportunities to tune their photochemical behavior and photophysical, spectroscopic and redox properties. This variation, involving also the α-diimine ligand as another option, is aimed to drastically change or, by contrast, only finely tune these properties according to the intended goals. The following practical applications of the complexes are of interest:

a) Source of reactive radicals (e.g. for medical application, such as cleavage of DNA chains, or for visible-light initiation of free radical photopolymerization).
b) Luminescence probes or sensors that exhibit long-lived emission or emission in the near-infrared region.

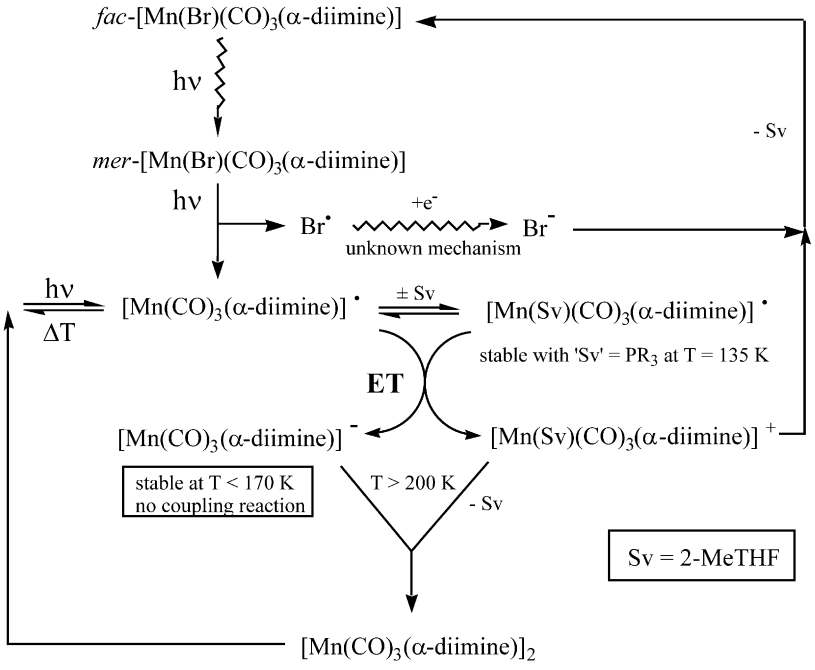

Scheme 1. Photochemical pathway of the complexes *fac*- and *mer*-[Mn(Br)(CO)$_3$(α-diimine)] toward the anion [Mn(CO)$_3$(α-diimine)]$^-$ as the ultimate photoproduct at low temperatures. The latter complex is also produced by electrochemical two-electron reduction of *fac*-[Mn(Br)(CO)$_3$(α-diimine)].

c) Electrocatalysts or photocatalysts (e.g. for reduction of carbon dioxide).
d) Photo- or electrochromic materials.

In order to achieve these goals, the bonding properties and reactivity of these complexes in the ground state, excited states and different redox states, and the influence thereon of the coordinated ligands and variable complex geometry, must be all understood in great detail. The combination of experimental and theoretical studies is a powerful tool in this regard. The same applies for combined photochemical and electrochemical investigations. In this paper it will be shown with several different examples of *trans*,*cis*-[Ru(X)(X′)-$(CO)_2$(α-diimine)] complexes which differences and common points exist between their photochemical and electrochemical activation and how their properties and reactivity in this regard respond to the variation of the axial X and X′ ligands. The structures of the complexes studied and examples of α-diimine ligands used are schematically depicted in Fig. 1.

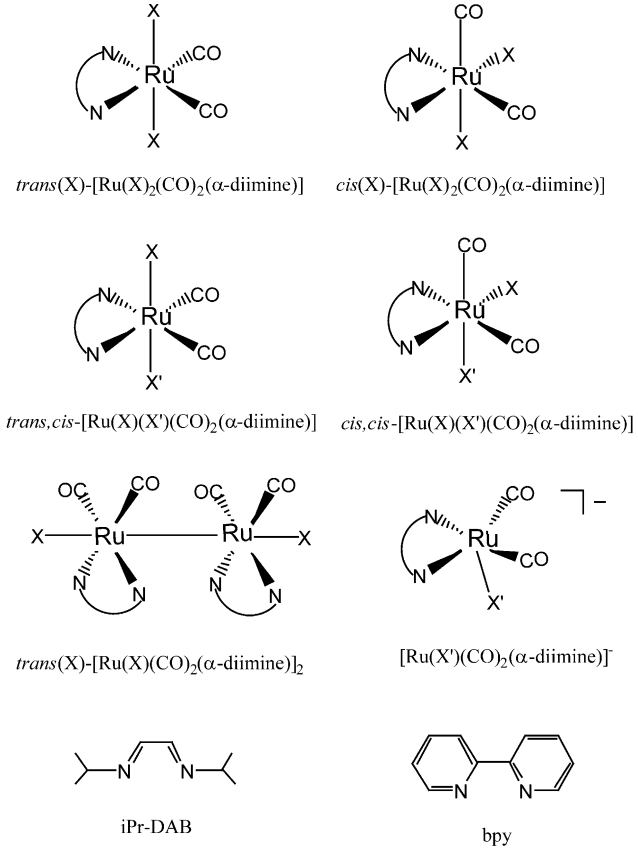

Fig. 1. Schematic molecular structures of the reviewed ruthenium complexes and the α-diimine ligands employed.

2. Experimental

2.1. Materials and preparations

Solvents, all of analytical grade, were freshly distilled under a nitrogen atmosphere: tetrahydrofuran (THF, Janssen) from a Na/benzophenone mixture, *n*-C_6H_{14} (Janssen) from a Na-wire, dichloromethane (CH_2Cl_2, Janssen) from P_2O_5, acetonitrile (MeCN, Janssen) and butyronitrile (*n*PrCN, Aldrich) from CaH_2. The supporting electrolyte Bu_4NPF_6 was dried overnight under vacuum at 80 °C. $P(OMe)_3$ (Aldrich) was distilled under reduced pressure from CaH_2. PPh_3 was recrystallized from EtOH/water at −30 °C. Ferrocene (Fc, BDH), bipyridine (bpy, Merck) and silver triflate AgOtf (Aldrich; $Otf^- = CF_3SO_3^-$) were used as received.

The ligand *N*,*N*′-diisopropyl-1,4-diaza-1,3-butadiene (*i*Pr-DAB) was synthesized according to a literature procedure [56]. The preparation of the complexes *trans*,*cis*-[Ru(X)(X′)$(CO)_2$(α-diimine)] (X = Cl, I; X′ = Me, Et; α-diimine = *i*Pr-DAB, bpy) and *trans*,*cis*-[Ru(Otf)(Me)$(CO)_2$(*i*Pr-DAB)] was described earlier [57–59]. The complex *trans*,*cis*-[Ru(Otf)(Me)-$(CO)_2$(bpy)] was synthesized by the same procedure. The precursor complex *trans*,*cis*-[Ru(I)(Me)$(CO)_2$(bpy)] was dissolved in CH_2Cl_2 and stirred with an equimolar amount of AgOtf for 2 h. After removing the AgI precipitate, the solvent was evaporated under vacuum. IR (CH_2Cl_2): ν(CO) at 2041, 1971 cm^{-1}. ^{1}H-NMR ($CDCl_3$): 8.94 (d) (2 bpy–H3), 8.18 (t) (2 bpy–H4), 8.10 (d) (2 bpy–H6), 7.58 (2 bpy–H5), −0.91 (s) (3 CH_3).

Complex *trans*,*cis*-[Ru(PPh_3)(Me)$(CO)_2$(*i*Pr-DAB)]-Otf was prepared by stirring a solution of *trans*,*cis*-[Ru(Otf)(Me)$(CO)_2$(*i*Pr-DAB)] in CH_2Cl_2 with an excess of PPh_3 for 3 h at room temperature, followed by evaporation of the solvent under vacuum. The crude product was purified by column chromatography on Silica 60 (Merck), activated by heating overnight under vacuum at 180 °C, with gradient elution by *n*-C_6H_{14}/THF. The fraction from *n*-C_6H_{14}/THF (50:50) was collected and recrystallized from CH_2Cl_2. The total yield was ca. 90%. IR (CH_2Cl_2): ν(CO) at 2045, 1987 cm^{-1}. ^{1}H-NMR ($CDCl_3$): 8.70 (d) (2 imine–CH), 7.51 (m) (12 Ph–H), 7.30 (m) (3 Ph–H), 3.84 (m) (2 *i*Pr–CH), 1.25 (d) (6 *i*Pr–CH_3), 0.80 (d) (6 *i*Pr–CH_3), 0.23 (d) (3 CH_3). Anal. Calc. (Found) for $C_{30}H_{34}F_3N_2O_2$-PRuS: C, 48.79 (49.38); H, 4.75 (4.66); N, 3.84 (3.84); P, 3.71 (3.39)%.

2.1.1. Spectroscopic and spectro-electrochemical measurements

FTIR spectra were recorded on a Bio-Rad FTS-7 spectrometer (eight scans, resolution of 2 cm^{-1}), electronic absorption spectra on a software-updated Perkin–Elmer Lambda 5 UV–vis spectrophotometer, and ^{1}H-NMR spectra on a Bruker AMX 300 spectro-

Table 1
Electrode potentials for reduction of the reviewed ruthenium carbonyl α-diimine complexes

Complex	E (V) vs. Fc/Fc^+	Reference
trans(Cl)-[$Ru(Cl)_2(CO)_2(bpy)$]	−1.60 [a]	[71,73] [e]
	−1.69 [a]	[74] [e]
trans(Cl)-[$Ru(Cl)(CO)_2(bpy)]_2$	−1.55 [a]	[74] [e]
[{$Ru(Cl)(CO)_2(bpy)\}_2$(μ-{$Ru(CO)_2(bpy)\}_2$)] (see Eq. (16))	−1.69 [a]	[74] [e]
trans(CH_3CN)-[$Ru(CH_3CN)_2(CO)_2(bpy)]^{2+}$	−1.29 [a]	[70] [e]
trans(CH_3CN)-[$Ru(CH_3CN)(CO)_2(bpy)]_2^{2+}$	−1.33 [a]	[72] [e]
trans,*cis*-[Ru(Cl){C(O)OMe}$(CO)_2$(bpy)]	−1.87 [a]	[73] [e]
trans{C(O)OMe}-[Ru{C(O)OMe}$(CO)_2(bpy)]_2$	−2.07 [b]	[73,74] [e]
trans,*cis*-[Ru(I)(Me)$(CO)_2$(bpy)]	−1.99 [a]	This work
	−1.93 [b]	
'[$Ru(Me)(CO)_2(bpy)]_2$'	−2.22 [b]	This work
trans,*cis*-[$Ru(Me)(PPh_3)(CO)_2(bpy)]^+$	−1.73 [b]	This work
trans,*cis*-[$Ru(Me)(PPh_3)(CO)_2(bpy)]^•$	−2.40 [a]	This work
trans,*cis*-[Ru(Me)(THF)$(CO)_2$(bpy)]$^+$	−1.76 [b]	This work
trans,*cis*-[Ru(Me)(THF)$(CO)_2$(bpy)]$^•$	−2.55 [a]	This work
trans(I)-[$Ru(I)_2(CO)_2$(*i*Pr-DAB)]	−1.40 [a]	[93]
trans,*cis*-[Ru(Me)(I)$(CO)_2$(*i*Pr-DAB)]	−1.55 [a]	This work
trans(Me)-[$Ru(Me)(CO)_2$(*i*Pr-DAB)$]_2$	−1.88 [a]	This work
trans,*cis*-[Ru(Me)(PrCN)$(CO)_2$(*i*Pr-DAB)]$^+$	−1.34 [b]	This work
trans,*cis*-[Ru(Me)(PrCN)$(CO)_2$(*i*Pr-DAB)]$^•$	−2.56 [a]	This work
trans,*cis*-[$Ru(Me)(PPh_3)(CO)_2$(*i*Pr-DAB)]$^+$	−1.16 [b]	This work
trans,*cis*-[$Ru(Me)(PPh_3)(CO)_2$(*i*Pr-DAB)]$^•$	−2.23 [a]	This work
trans,*cis*-[Ru(Cl)($SnPh_3$)$(CO)_2$(*i*Pr-DAB)]	−1.48 [a]	[77]
trans($SnPh_3$)-[$Ru(SnPh_3)(CO)_2$(*i*Pr-DAB)$]_2$	−1.68 [a]	[77]
trans,*cis*-[Ru(Cl)($PbPh_3$)$(CO)_2$(*i*Pr-DAB)]	−1.60 [a]	[77]
trans($PbPh_3$)-[$Ru(PbPh_3)(CO)_2$(*i*Pr-DAB)$]_2$	−1.77 [a]	[77]
trans($SnPh_3$)-[$Ru(SnPh_3)_2(CO)_2$(*i*Pr-DAB)]	−1.86 [b]	[77]
trans($SnPh_3$)-[$Ru(SnPh_3)_2(CO)_2$(*i*Pr-DAB)]$^{•-}$	< −2.8	[77,80]
trans,*cis*-[Ru(Me)($SnPh_3$)$(CO)_2$(*i*Pr-DAB)]	−1.92 [b]	[77]
trans,*cis*-[Ru(Me)($SnPh_3$)$(CO)_2$(*i*Pr-DAB)]$^{•-}$	−2.71 [a]	[77]
trans($PbPh_3$)-[$Ru(PbPh_3)_2(CO)_2$(*i*Pr-DAB)]	−1.69 [b]	[77]
trans($PbPh_3$)-[$Ru(PbPh_3)_2(CO)_2$(*i*Pr-DAB)]$^{•-}$	−2.31 [b]	[77]
trans,*cis*-[Ru($SnPh_3$)($GePh_3$)$(CO)_2$(*i*Pr-DAB)]	−1.72 [b]	[77]
trans,*cis*-[Ru($SnPh_3$)($GePh_3$)$(CO)_2$(*i*Pr-DAB)]$^{•-}$	−2.62 [a]	[77]
trans,*cis*-[Ru($SnPh_3$){$Ru(CO)_2Cp$}$(CO)_2$(*i*Pr-DAB)] [c]	−1.98 [a]	[85]
	−1.82 [b]	
trans{$Ru(CO)_2Cp$}-[Ru{$Ru(CO)_2Cp\}_2(CO)_2$(*i*Pr-DAB)] [d]	−2.04 [a]	[85]
	−2.05 [b]	

[a] Electrode potential of irreversible reduction, $E_{p,c}$ (dependent on kinetic parameters).
[b] Electrode potential of reversible reduction, $E_{1/2}$.
[c] This complex is reversibly oxidized in PrCN at 213 K; $E_{1/2} = 0.20$ V vs. Fc/Fc^+.
[d] This complex is reversibly oxidized in PrCN at 213 K; $E_{1/2} = -0.06$ V vs. Fc/Fc^+.
[e] Potential determined in the original paper vs 10^{-2} M Ag^+/Ag in CH_3CN. Conversion to the Fc/Fc^+ reference has been done by adding the value of −0.09 V [94].

meter. Elemental analyzes were carried out in the Microanalytisches Laboratorium of Dornis & Kolbe, Mülheim a.d. Ruhr, Germany.

IR and UV–vis spectroelectrochemical experiments at room and low temperatures were performed with OTTLE cells that have been described elsewhere [60,61]. The potential control was achieved with a PA4 (EKOM, Czech Republic) potentiostat. Solutions for the spectroelectrochemical experiments were carefully prepared under a nitrogen atmosphere using Schlenk techniques. They typically contained 3×10^{-1} M Bu_4NPF_6 and 10^{-2} M ruthenium complex.

Cyclic voltammetry was carried out with a PAR Model 283 potentiostat. Typically, 3 ml of a solution containing 10^{-1} M Bu_4NPF_6 and 5×10^{-4} M ruthenium complex were placed in a gas-tight single-compartment CV cell equipped with a at a Pt disk working (0.65 mm^2 real surface area). Ag wire pseudoreference and Pt gauze auxiliary electrodes. The ferrocenium/ferrocene (Fc^+/Fc) redox couple served as an internal standard

[62] for determination of redox potentials and electrochemical reversibility of the redox steps.

3. Results and discussion

The reduction potentials of the ruthenium complexes reviewed in this paper are summarized in Table 1.

3.1. The complex *trans*(Cl)-[Ru(Cl)$_2$(CO)$_2$(bpy)] and its derivatives

The lowest optically prepared excited state of the complex *trans*(Cl)-[Ru(Cl)$_2$(CO)$_2$(bpy)] possesses a predominant MLCT character [62–64]. Irradiation into the corresponding absorption band causes cleavage of a Ru–CO bond and rapid formation of *cis*(Cl)-[Ru(Cl)$_2$(CH$_3$CN)(CO)(bpy)] in acetonitrile or a Cl-bridged dinuclear complex [{Ru(Cl)(CO)(bpy)}$_2$(μ-Cl)$_2$] in dichloromethane [62,63]. It is interesting to note that the isomer *cis*(Cl)-[Ru(Cl)$_2$(CO)$_2$(bpy)] gives the same primary photoproduct *cis*(Cl)-[Ru(Cl)$_2$-(CH$_3$CN)(CO)(bpy)] [63]. The isomerization step along the photochemical pathway of *trans*(Cl)-[Ru(Cl)$_2$-(CO)$_2$(bpy)] in acetonitrile probably occurs after the release of an equatorial carbonyl ligand, giving rise to the fluxional five-coordinate transient [Ru(Cl)$_2$(CO)-(bpy)] that concomitantly moves a chloride to the equatorial plane and binds a solvent molecule at the free axial site [64]. In this respect the photochemical pathway (dissociative substitution) of *trans*(Cl)-[Ru(Cl)$_2$(CO)$_2$(bpy)] resembles those of *trans*,*cis*-[Ru(Me)(I)(CO)$_2$(α-diimine)] [65,66] and *fac*-[Mn(Br)-(CO)$_3$(α-diimine)] [50,67] (α-diimine = e.g. bpy). The photoisomerization of the latter complex into *mer*-[Mn(Br)(CO)$_3$(α-diimine)] proceeds via the transient complexes [Mn(Br)(CO)$_2$(α-diimine)] and *cis*,*cis*-[Mn(Br)(Sv)(CO)$_2$(α-diimine)] (Sv = donor solvent). DFT MO calculations by Rosa et al. on model compounds *fac*-[Mn(Br)(CO)$_3$(H-DAB)] and [Mn(Br)-(CO)$_2$(H-DAB)] dealt with the primary step of this photoreaction that was shown to involve dissociation of an equatorial CO ligand followed by movement of the Br ligand to this open coordination site [68]. The theoretical description of the latter relaxation process still needs support from experimental studies. However, differently from the unstable complexes *mer*-[Mn(Br)(CO)$_3$(α-diimine)] that thermally isomerize back to the *fac*-precursor and upon visible irradiation undergo homolytic cleavage of the Mn–Br bond [50], the photoproduct *cis*(Cl)-[Ru(Cl)$_2$(CH$_3$CN)(CO)(bpy)] is thermally stable and its illumination with near-UV light gives rise to the formation of [Ru(Cl)$_2$(CH$_3$CN)$_2$(bpy)] [62]. More details about the photosubstitution paths of *trans*(Cl)- and *cis*(Cl)-[Ru(Cl)$_2$(CO)$_2$(bpy)], in particular the primary photodissociation of Cl, may be inferred from so far neglected ultrafast (fs-ps) time-resolved spectroscopic studies of these isomers [69].

Consistent with the CO dissociation in the MLCT excited state, electrochemical one-electron oxidation of *trans*(Cl)-[Ru(Cl)$_2$(CO)$_2$(bpy)] also causes cleavage of a Ru–CO bond [70]. However, this reaction is associated with the loss of a Cl ligand, ultimately producing [Ru(Cl)(CO)(CH$_3$CN)$_2$(bpy)]$^{2+}$ (Eqs. (8)–(10)). The latter product is reversibly reduced to [Ru(Cl)(CO)-(CH$_3$CN)$_2$(bpy)]$^+$ which is again photoreactive and, similarly to the parent complex *trans*(Cl)-[Ru(Cl)$_2$-(CO)$_2$(bpy)], it converts upon MLCT photoexcitation into [Ru(Cl)(CH$_3$CN)$_3$(bpy)]$^+$. This behavior is different from that of the recently studied complex *trans*(Cl)-[Os(Cl)$_2$(CO)$_2$(bpy)] with stronger Os–CO and Os–Cl bonds, which oxidizes to less thermaly reactive *trans*(Cl)-[Os(Cl)$_2$(CO)$_2$(bpy)]$^+$ and [Os(Cl)$_2$(CO)(CH$_3$-CN)(bpy)]$^+$. Reverse one-electron reduction of the latter complex results in the photostable CO-substituted product [Os(Cl)$_2$(CO)(CH$_3$CN)(bpy)] possessing a mixed MLCT/XLCT lowest excited state, as revealed by resonance Raman spectroscopy [38].

$$\textit{trans}\text{(Cl)-[Ru(Cl)}_2\text{(CO)}_2\text{(bpy)]} \rightarrow \textit{trans}\text{(Cl)-[Ru(Cl)}_2\text{(CO)}_2\text{(bpy)]}^+ + e^- \quad (8)$$

$$\textit{trans}\text{(Cl)-[Ru(Cl)}_2\text{(CO)}_2\text{(bpy)]}^+ \rightarrow [\text{Ru(Cl)}_2\text{(CO)(bpy)}]^+ + \text{CO} \quad (9)$$

$$[\text{Ru(Cl)}_2\text{(CO)(bpy)}]^+ + 2\ \text{CH}_3\text{CN} \rightarrow [\text{Ru(Cl)(CO)(CH}_3\text{CN)}_2\text{(bpy)}]^{2+} + \text{Cl}^- \quad (10)$$

The electrochemical reduction path of *trans*(Cl)-[Ru(Cl)$_2$(CO)$_2$(bpy)] is remarkably different from those of the other *trans*,*cis*-[Ru(X)(X′)CO)$_2$(α-diimine)] complexes (vide infra). Consistently with the nature of the lowest unoccupied orbital, the primary one-electron reduction step is localized largely on the bpy ligand, producing the radical anion *trans*(Cl)-[Ru^{II}(Cl)$_2$(CO)$_2$(bpy)]$^{\bullet -}$. This species rapidly loses a Cl$^-$ ligand and converts to the transient five-coordinate radical [Ru^I(Cl)(CO)$_2$(bpy)]$^\bullet$ that readily dimerizes (Eqs. (11)–(13)) [71]. There has been no evidence from cyclic voltammetric or spectroelectrochemical experiments that [Ru^I(Cl)(CO)$_2$(bpy)]$^\bullet$ undergoes further reduction to the corresponding five-coordinate anion in competition with dimerization. Most important, independent experiments have proven that the dimer *trans*(Cl)-[Ru(Cl)(CO)$_2$(bpy)]$_2$ is reducible, probably again at a bpy ligand, at the applied cathodic potential of the parent *trans*-dichloro complex (see data in Table 1) and expels another Cl$^-$ ligand [72]. Consequently, the reduction pathway proceeds via the formation of a tetramer [{Ru(Cl)(CO)$_2$(bpy)}$_2$(μ-{Ru(CO)$_2$(bpy)}$_2$)] towards higher oligomers until a polymeric chain [Ru(CO)$_2$(bpy)]$_n$ is obtained as the ultimate 2n-electron reduced Ru(0) species (Eqs. (14)–(17)) [73]. Also

$[Ru(CO)_2(bpy)]_n$, deposited as an insoluble air-sensitive film on the cathode, can be further reduced at a limited number of bpy ligands (ca. 3% $[bpy]^{\bullet -}$ doping level) (Eq. (18)). This step is chemically reversible and initiates an efficient electrocatalytic reduction of carbon dioxide with this remarkable compound [71]. Recent studies reveal that $[Ru(CO)_2(bpy)]_n$ also results from the reduction of the isomer *cis*(Cl)-$[Ru(Cl)_2(CO)_2(bpy)]$ [74].

The same reduction pathway leading to $[Ru(CO)_2(bpy)]_n$ also operates for other complexes *trans*(X)-$[Ru(X)_2(CO)_2(bpy)]^n$ ($n = 0, +2$) with readily leaving ligands X, such as acetonitrile (see Table 1) or thiocyanate, acetate and triflate [71]. In sharp contrast, no electropolymerization was observed for *trans*,*cis*-$[Ru(Cl)\{C(O)OMe\}(CO)_2(bpy)]$ with the firmly bound methoxycarbonyl ligand (see Table 1), [73,74] and for the *trans*(Cl)-dichloro complex with the bpy ligand bearing strongly electron-withdrawing nitro substituents [75].

$$trans\text{(Cl)-}[Ru(Cl)_2(CO)_2(bpy)] + e^- \rightarrow trans\text{(Cl)-}[Ru(Cl)_2(CO)_2(bpy)]^{\bullet -} \quad (11)$$

$$trans\text{(Cl)-}[Ru(Cl)_2(CO)_2(bpy)]^{\bullet -} \rightarrow [Ru(Cl)(CO)_2(bpy)]^{\bullet} + Cl^- \quad (12)$$

$$2\,[Ru(Cl)(CO)_2(bpy)]^{\bullet} \rightarrow [Ru(Cl)(CO)_2(bpy)]_2 \quad (13)$$

$$[Ru(Cl)(CO)_2(bpy)]_2 + e^- \rightarrow [(bpy)(CO)_2(Cl)Ru\text{–}Ru(Cl)(CO)_2(bpy^{\bullet -})]^- \quad (14)$$

$$[(bpy)(CO)_2(Cl)Ru\text{–}Ru(Cl)(CO)_2(bpy^{\bullet -})]^- \rightarrow [(bpy)(CO)_2(Cl)Ru\text{–}Ru(CO)_2(bpy^{\bullet -})] + Cl^- \quad (15)$$

$$2\,[(bpy)(CO)_2(Cl)Ru\text{–}Ru(CO)_2(bpy^{\bullet -})] \rightarrow [\{Ru(Cl)(CO)_2(bpy)\}_2(\mu\text{-}\{Ru(CO)_2(bpy)\}_2)] \quad (16)$$

$$n\ trans\text{(Cl)-}[Ru(Cl)_2(CO)_2(bpy)] + 2ne^- \rightarrow [Ru(CO)_2(bpy)]_n + 2nCl^- \quad (17)$$

$$[Ru(CO)_2(bpy)]_n + xe^- \rightarrow [Ru_n(CO)_{2n}(bpy)_{n-x}(bpy^{\bullet -})_x]^{x-} \quad (18)$$

($x = $ ca. $0.03n$)

3.2. Complexes *trans*(I)-[Ru(I)$_2$(CO)$_2$(*i*Pr-DAB)] and *trans*,*cis*-[Ru(Cl)(X′)(CO)$_2$(*i*Pr-DAB)] (X′ = SnPh$_3$, PbPh$_3$)

Scarce literature data on *trans*(I)-$[Ru(I)_2(CO)_2(i$Pr-DAB)] point to a similarity between the photochemistry of this complex and that of the bpy-compounds *trans*(Cl)-$[Ru(Cl)_2(CO)_2(bpy)]$ and *trans*(X)-$[Ru(X)_2(CO)_2$(dcbpy)] (X = Br, I; dcbpy = 4,4′-dicarboxylic acid-2,2′-bipyridine) [64,71]. Thus, irradiation of the *i*Pr-DAB compound with visible light in acetonitrile induces an efficient CO substitution reaction and results in *trans*(I)-$[Ru(I)_2(CO)(CH_3CN)(i$Pr-DAB)] (ν(CO) at 1975 cm^{-1}), probably via a dissociative pathway [76]. On the other hand, a poorly soluble complex $[Ru(I)_2(CO)(i$Pr-DAB)]$_n$ is formed by photolysis in dichloromethane [76] as the equivalent of the Cl-bridged dimer $[\{Ru(Cl)(CO)(bpy)\}_2(\mu\text{-}Cl)_2]$ [63]. The cleavage of a Ru–CO bond likely occurs upon initial population of a XLCT (I-to-*i*Pr-DAB charge transfer) excited state of *trans*(I)-$[Ru(I)_2(CO)_2(i$Pr-DAB)]. Electrochemical reduction of this complex is again an irreversible two-electron process, resulting in dissociation of the iodide ligands and concomitant formation of the reactive anion $[Ru(I)(CO)_2(i$Pr-DAB)]$^-$ and a Ru(0) complex [Ru(Sv)(CO)$_2$(*i*Pr-DAB)] (Sv = donor solvent; it can easily be replaced by e.g. PPh_3) (Eqs. (19)–(22)) [76]. It can be reasonably expected that the photochemical reactivity and the reduction pathway of *trans*(Cl)-$[Ru(Cl)_2(CO)_2(i$Pr-DAB)] is similar. The close resemblance between the photochemistry and electrochemistry of complexes with bpy and *i*Pr-DAB ligands is not exceptional. As another example may serve the compounds *fac*-$[Mn(X)(CO)_3(\alpha$-diimine)] (X = Cl, Br; α-diimine = bpy, *i*Pr-DAB) [47,67].

$$trans\text{(I)-}[Ru(I)_2(CO)_2(i\text{Pr-DAB})] + e^- \rightarrow trans\text{(I)-}[Ru(I)_2(CO)_2(i\text{Pr-DAB})]^{\bullet -} \quad (19)$$

$$trans\text{(I)-}[Ru(I)_2(CO)_2(i\text{Pr-DAB})]^{\bullet -} \rightarrow [Ru(I)(CO)_2(i\text{Pr-DAB})]^{\bullet} + I^- \quad (20)$$

$$[Ru(I)(CO)_2(i\text{Pr-DAB})]^{\bullet} + e^- \rightarrow [Ru(I)(CO)_2(i\text{Pr-DAB})]^- \quad (21)$$

$$[Ru(I)(CO)_2(i\text{Pr-DAB})]^- + Sv \rightarrow [Ru(Sv)(CO)_2(i\text{Pr-DAB})] + I^- \quad (22)$$

Replacement of a Cl^- ligand in *trans*(Cl)-$[Ru(Cl)_2(CO)_2(i$Pr-DAB)] with strongly σ-bonded groups such as $SnPh_3^-$ or $PbPh_3^-$ has pronounced consequences both for the nature of the lowest excited state and for the reduction pathway. Spectroscopic studies (emission and ns time-resolved IR spectra) and DFT calculations on model complexes have confirmed that the lowest excited state obtained a mixed XLCT/MLCT (X = Cl, L = *i*Pr-DAB) character due to an antibonding $\pi^*\{4d_\pi(Ru)/3p(Cl)\}$ character of the highest occupied molecular orbital (HOMO). The lowest unoccupied molecular orbital mainly resides on the π^*(*i*Pr-DAB) system [39]. In this excited state the complexes are photostable, the Ru–CO bonding being little affected by the merely partial oxidation of the metal center. In this regard they bear strong resemblance to other photostable complexes *trans*(Cl)-$[Os(Cl)_2(CH_3CN)(CO)(bpy)]$ and *trans*,*cis*-$[Ru(Cl)\{C(O)OMe\}(CO)_2(bpy)]$. Similar to the latter compound, electrochemical reduction of *trans*,*cis*-$[Ru(Cl)(X')(CO)_2(i$Pr-DAB)] (X′ = $SnPh_3$, $PbPh_3$) does not induce loss of the ligand and, hence, polymerization. The reduction pathway, summarized in Scheme 2, was thoroughly investigated by several electrochemical and spectroelectrochemical techniques at variable temperatures [77].

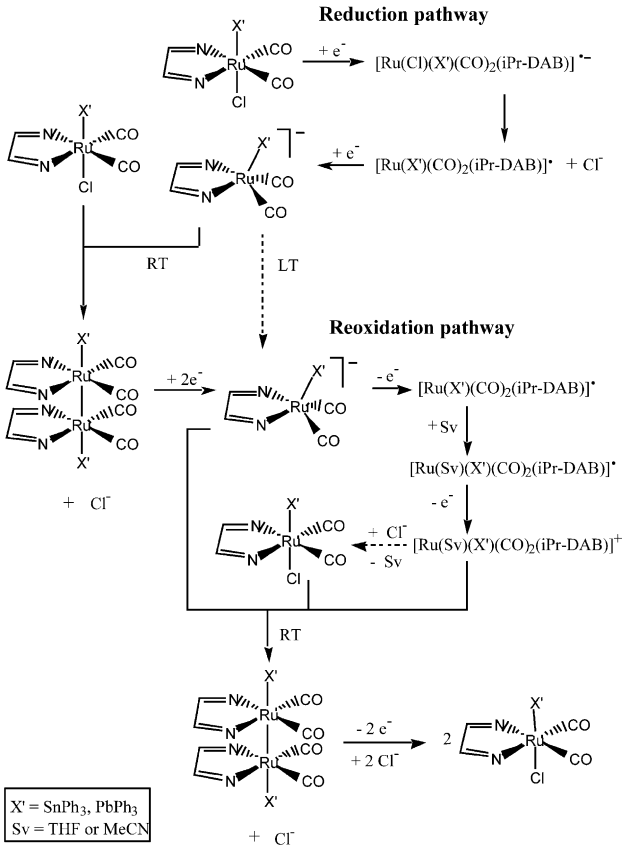

Scheme 2. Reduction pathway of the inorganometallic complexes *trans*,*cis*-[Ru(Cl)(X′)(CO)$_2$(*i*Pr-DAB)] (X′ = $SnPh_3$, $PbPh_3$) described in Section 3.2.

The initially produced radical anions rapidly lose the weakly bound Cl^- ligand. Differently from the reduction pathway of *trans*(Cl)-[Ru(Cl)$_2$(CO)$_2$(bpy)], the stronger Ru–X′ bond remains intact. Further, the five-coordinate radicals [Ru(X′)(CO)$_2$(*i*Pr-DAB)]$^\bullet$ (X′ = $SnPh_3$, $PbPh_3$) are reduced less negatively than the corresponding parent complexes, which prevents their direct dimerization in the vicinity of the cathode (in contrast to the situation observed for X′ = Me, see Section 3.5); instead, the reduction gives rise to the instantaneous formation of the five-coordinate anions [Ru(X′)(CO)$_2$(*i*Pr-DAB)]$^-$. At room temperature, a zero-electron coupling reaction between the anion [Ru(X′)(CO)$_2$(*i*Pr-DAB)]$^-$ and the yet non-reduced parent complex produces ultimately the dimer *trans*(X′)-[Ru(X′)(CO)$_2$(*i*Pr-DAB)]$_2$. Cyclic voltammetry has shown that this coupling reaction becomes completely inhibited at temperatures below 223 K. The latter dimeric complex is reduced at a more negative electrode potential back to the anion [Ru(X′)(CO)$_2$(*i*Pr-DAB)]$^-$ (Table 1), closely resembling the derivatives with X′ = Me and Et, discussed hereinafter. The five-coordinate geometry of the anions is stabilized by an extensively delocalized π-bonding within the Ru(*i*Pr-DAB) metallacycle that was proven by thorough analysis of their ^{1}H-, ^{13}C-, ^{119}Sn-NMR and resonance Raman spectra [77].

It can be concluded that the reduction pathways of the complexes *trans*,*cis*-[Ru(Cl)(X′)(CO)$_2$(*i*Pr-DAB)] (X′ = $SnPh_3$, $PbPh_3$) and *fac*-[Mn(X)(CO)$_3$(*i*Pr-DAB)] (X = halide) [47] are qualitatively identical, involving release of the halide ligand in the one-electron reduced state. The resulting five-coordinate radicals with strongly delocalized Mn(*i*Pr-DAB) π-system are capable of easy accommodation of another electron, hence being reducible less negatively than the parent complexes. In contrast to the ruthenium complexes, the managnese compounds are photolabile and undergo a dissociative isomerization induced by Mn–CO bond cleavage.

The reverse reoxidation pathway of the anions [Ru(X′)(CO)$_2$(*i*Pr-DAB)]$^-$ toward the parent complexes *trans*,*cis*-[Ru(Cl)(X′)(CO)$_2$(*i*Pr-DAB)] (X′ = $SnPh_3$, $PbPh_3$) shows many similarities with the reduction pathway. It is also schematically depicted in Scheme 2. Note the important role of the donor solvent Sv that, differently from the reduction pathway, this time well coordinates to the transient five-coordinate radical [Ru(X′)(CO)$_2$(*i*Pr-DAB)]$^\bullet$, inducing its one-electron oxidation prior to the recoordination of the chloride ligand [77].

It is noteworthy that the complex *trans*,*cis*-[Ru(Cl)($SnPh_3$)(CO)$_2$(*i*Pr-DAB)] was examined as a catalyst precursor for the electrocatalytic reduction of carbon dioxide [78]. The five-coordinate anion [Ru($SnPh_3$)(CO)$_2$(*i*Pr-DAB)]$^-$ was identified as the active species in this process that converted carbon dioxide into free CO, CO_3^{2-} and HCO_2^-. The yield of these products was low due to gradual decomposition of [Ru($SnPh_3$)(CO)$_2$(*i*Pr-DAB)]$^-$ into an inactive air-stable red complex (ν(CO) at 1987, 1921 cm^{-1} (THF, 293 K); 1990, 1923 cm^{-1} (benzene, 293 K)) that may electronically resemble the dimer [Ru(CO)$_2$(*i*Pr-DAB)]$_2$ reported by Staal et al. (ν(CO) at 1980, 1922 cm^{-1} (C_6H_{14}, 293 K)). The two Ru(CO)$_2$ groups in the latter complex are connected by the *i*Pr-DAB ligands forming σ*N*,σ*N*′,η^2-C=N-bound bridges [79].

3.3. Complexes *trans*,*cis*-[Ru(X)(X′)(CO)$_2$(*i*Pr-DAB)] (X = $SnPh_3$, $PbPh_3$; X′ = Me, $SnPh_3$, $PbPh_3$, $GePh_3$)

These compounds represent a very interesting class of inorganometallic complexes with strongly delocalized covalent three-center, four-electron X–Ru–X′ σ-bond and Ru(*i*Pr-DAB) π-system. Thus, as revealed by DFT calculations and in full agreement with various experimental spectroscopic data, the HOMO possesses a major contribution from the antisymmetric combination {sp^3(X) − sp^3(X′)} + p$_z$(Ru), to a minor extent also residing on the π*(*i*Pr-DAB) system. The lowest unoccupied molecular orbital is predominantly the π*(*i*Pr-

DAB) orbital, with some $\{sp^3(X)-sp^3(X')\}+d_{yz}(Ru)$ contribution [80–82]. The lowest optically accessible excited state of these complexes therefore obtains a predominant σ(X–Ru–X′)-to-π*(*i*Pr-DAB) character. Most striking features of this $^3\sigma\pi$ (or ^{3}SBLCT) excited state are its long lifetime (up to ms) and strong emission [39,83]. Most of these complexes were found to be photochemically weakly reactive and undergo relatively slow homolysis of the Ru–X′ bond on a microsecond time scale. Only the complex with $X = X' = PbPh_3$ probably undergoes photoisomerization, similar to some complexes *trans*,*cis*-[Ru(X)(X′)(CO)$_2$(*i*Pr-DAB)] (X = halide, X′ = alkyl). Notably, it is always the weaker one of the Ru–X and Ru–X′ bonds of the asymmetric X–Sn–X′ combinations that is homolytically split upon irradiation; e.g. the Ru–Me bond for Ph_3Sn–Ru–Me. In *trans*,*cis*-[Ru($SnPh_3$)($GePh_3$)(CO)$_2$(*i*Pr-DAB)] the Ru–Sn and Ru–Ge bonds are comparably strong and, indeed, both $SnPh_3$ and $GePh_3$ ligands are released upon irradiation [84]. Interestingly, this behavior can also be observed upon electrochemical reduction of these complexes. For example, two-electron reduction of *trans*,*cis*-[Ru($SnPh_3$)($GePh_3$)(CO)$_2$(*i*Pr-DAB)] (vide infra) produces both anions [Ru(X)(CO)$_2$(*i*Pr-DAB)]$^-$ (X = $SnPh_3$ and $GePh_3$) in approximately equal amounts [77].

The strong σπ* interaction in this class of complexes with strongly σ-bonded ligands is responsible for the considerable negative shift of their reduction potentials compared to other *i*Pr-DAB complexes listed in Table 1, i.e. *trans*,*cis*-[Ru(Me)(I)(CO)$_2$(*i*Pr-DAB)] with the lower-lying LUMO localized predominantly on the π*(*i*Pr-DAB) system. The one-electron reduction of all these complexes produces corresponding radical anions *trans*,*cis*-[Ru(X)(X′)(CO)$_2$(*i*Pr-DAB)]$^{\bullet -}$ (X = $SnPh_3$, $PbPh_3$; X′ = Me, $SnPh_3$, $PbPh_3$, $GePh_3$) that are stable already at room temperature [77,80]. Slow dissociation of the X$^-$ ligand was only observed during spectroelectrochemical experiments for the complexes *trans*,*cis*-[Ru($SnPh_3$)(Me)(CO)$_2$(*i*Pr-DAB)]$^{\bullet -}$ (X = Me) and *trans*,*cis*-[Ru($PbPh_3$)($GePh_3$)(CO)$_2$(*i*Pr-DAB)] (X = $PbPh_3$). In this case the reduction of the parent complexes produced the correspondig five-coordinate anions [Ru(X′)(CO)$_2$(*i*Pr-DAB)]$^-$ via the ECE pathway, involving the coordinatively unsaturated radical transients (Scheme 3) [77]. The anions [Ru(X′)(CO)$_2$-(*i*Pr-DAB)]$^-$ as the ultimate two-electron reduced products are also formed upon the reduction of the stable radical anions *trans*,*cis*-[Ru(X)(X′)(CO)$_2$(*i*Pr-DAB)]$^{\bullet -}$ to the corresponding dianion, followed by fast dissociation of the X$^-$ ligand (the EEC pathway in Scheme 3).

The bonding properties of these interesting reduction products were studied by several spectroscopic techniques, for example EPR spectroscopy, and by DFT MO calculations [77,80]. EPR parameters of the radical anions *trans*,*cis*-[Ru(X)(X′)(CO)$_2$(*i*Pr-DAB)]$^{\bullet -}$ are summarized in Table 2. As an example, the intriguing EPR spectrum of *trans*,*cis*-[Ru($SnPh_3$)($GePh_3$)-(CO)$_2$(*i*Pr-DAB)]$^{\bullet -}$ is depicted in Fig. 2. It is worth mentioning that values of the corresponding EPR *g*-factors, decreasing for the X/X′ combinations in the order $Me/SnPh_3 > SnPh_3/GePh_3 > SnPh_3/SnPh_3 > PbPh_3/PbPh_3$, nicely correlate with the decreasing energetic separation between the singly occupied molecular orbital (SOMO) and the LUMO in the radical anions. The latter parameter was obtained by UV–vis spectroscopy from the energetic position of the characteristic lowest-lying absorption band belonging to the SOMO → LUMO electronic transition [80].

3.4. Complexes *trans*,*cis*-[Ru(X)(X′)(CO)$_2$(*i*Pr-DAB)] (X = Ru(CO)$_2$Cp; X′ = $SnPh_3$, Ru(CO)$_2$Cp)

The title complexes possess the same highly delocalized dissociative ^{3}SBLCT (or $^3\sigma\pi^*$) excited state as the inorganometallic complexes reported in Section 3.3. Population of this state therefore results in the homolytic cleavage of a Ru–Ru(Cp) bond as the primary photoprocess, with the formation of corresponding radicals that react further thermally. Compared with the complexes in Section 3.3, the notable differences concern the more efficient metal–metal bond cleavage,

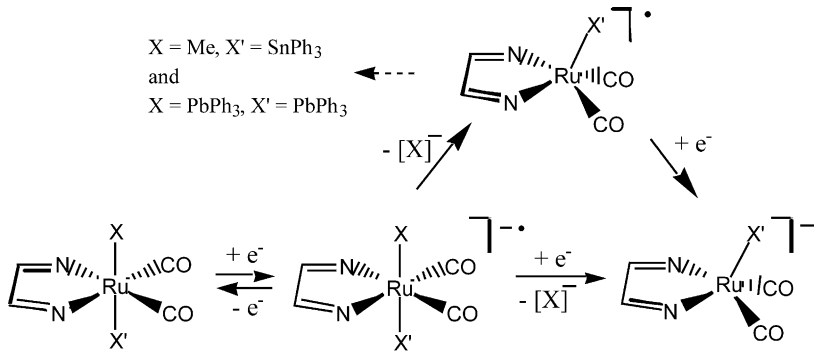

Scheme 3. Reduction pathway of the inorganometallic complexes *trans*,*cis*-[Ru(X)(X′)(CO)$_2$(*i*Pr-DAB)] (X = $SnPh_3$, $PbPh_3$; X′ = Me, $SnPh_3$, $PbPh_3$, $GePh_3$) described in Section 3.3.

Table 2
EPR parameters of inorganometallic radical anions *trans*,*cis*-[Ru(X)(X′)(CO)$_2$(*i*Pr-DAB)]$^{\bullet -}$

Nuclei	No.	Natural abundance (%)	Spin	A_{iso} (G) [f]	X = $SnPh_3$, X′ = $SnPh_3$ (G) [a]	X = $GePh_3$, X′ = $SnPh_3$ (G) [a]	X = Me, X′ = $SnPh_3$ (G) [a]	X = $PbPh_3$, X′ = $PbPh_3$ (G) [a]
^{99}Ru	1	12.7	5/2		5.7	5.34	[e]	[e]
^{101}Ru	1	17.1	5/2		6.4	6.00	[e]	[e]
^{117}Sn	1 or 2	7.6	1/2	−6669	317	350	~370	
^{117}Sn/A_{iso}					0.047	0.052	~0.055	
^{119}Sn	1 or 2	8.6	1/2	−7268	332	366	~370	
^{117}Sn/A_{iso}					0.047	0.050	~0.055	
^{207}Pb	1 or 2	22.6	1/2	+6868				~570
^{207}Pb/A_{iso}								0.083
^{73}Ge	1	7.6	9/2	−535		14.6		
^{73}Ge/A_{iso}						0.027		
^{14}N	2	99.6	1		8.20	8.00	7.95	~7.5 [e]
^{1}H [b]	2	99.9	1/2		3.55	4.29	3.62	~4.0 [e]
^{1}H [c]	2	99.9	1/2		3.25	3.71	2.69	~3.3 [e]
^{1}H [d]	3	99.9	1/2				0.68	
g-factor					1.9960	1.9968	1.9986	1.9919

[a] Hyperfine coupling constants based on simulated values, except the $^{117/119}$Sn and ^{207}Pb hyperfine coupling constants that have been derived from the experimental spectra.
[b] Imine protons.
[c] ($CH(CH_3)_2$.
[d] Ru–CH_3.
[e] These values could not be (accurately) determined due to a large natural line width or poor signal-to-noise ratio.
[f] A_{iso}, theoretical isotropic coupling constants for free ions.

emission shifted to the NIR region due to lower oxidation potentials, and shorter emission lifetimes [83].

The electrochemical reduction of the complexes produces intially the corresponding radical anions *trans*,*cis*-[Ru(X)(X′)(CO)$_2$(*i*Pr-DAB)]$^{\bullet -}$ (X = $Ru(CO)_2Cp$; X′ = $SnPh_3$, $Ru(CO)_2Cp$). In agreement with the more pronounced photoreactivity of the parent complexes in the lowest excited state, these radical anions are significantly shorter-lived at room temperature than those from Section 3.3, and difficult to be observed spectroscopically. Similar to the photoreactions, the instability of the radical anions results in the cleavage of a Ru–Ru(Cp) bond, giving rise to the dissociation of the reactive radical fragment

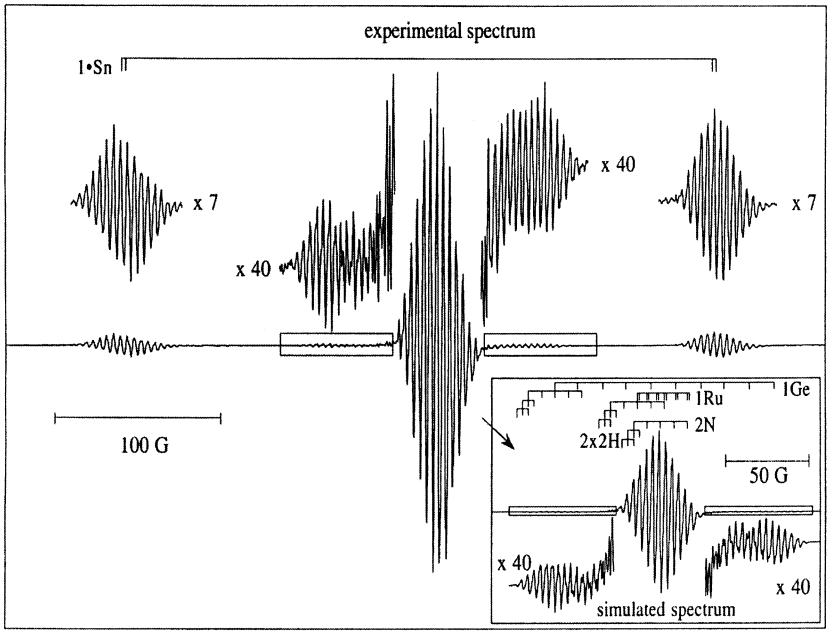

Fig. 2. Experimental and simulated EPR spectrum of *trans*,*cis*-[Ru($SnPh_3$)($GePh_3$)(CO)$_2$(*i*Pr-DAB)]$^{\bullet -}$ described in Section 3.3 (Na^+ salt, THF, room temperature).

$[Ru(CO)_2Cp]^{\bullet}$ and the formation of the corresponding anions $[Ru(SnPh_3)(CO)_2(i\text{Pr-DAB})]^-$ and unstable $[Ru\{Ru(CO)_2Cp\}(CO)_2(i\text{Pr-DAB})]^-$ [85].

The main reason why these Ru–Ru(Cp) bonded complexes are treated separately regards their remarkable oxidation pathway. As already mentioned above, both complexes exhibit less positive oxidation potentials, which imparts them with special photophysical properties, in particular the NIR emission. The reason for this difference is the presence of the strongly donating axial $Ru(CO)_2Cp$ group(s) that stabilize the one-electron oxidized state of the complexes. The stabilization is pronounced to such a degree that in the case of *trans*,*cis*-$[Ru\{Ru(CO)_2Cp\}_2(CO)_2(i\text{Pr-DAB})]$ the corresponding radical cations are even detectable at low temperatures , e.g. by in situ IR spectroscopy (see Fig. 3) [85].

The multistep electrochemical reduction and oxidation pathways of the title complexes are presented in Schemes 4 and 5.

3.5. Complexes *trans*,*cis*-[Ru(Me)(I)(CO)$_2$(α-diimine)] (α-diimine) = *i*Pr-DAB, bpy) and their derivatives: novel spectro-electrochemical results

The photochemical and photophysical properties of the complexes *trans*,*cis*-$[Ru(X')(X)(CO)_2$ (α-diimine)] (X = halide, X′ = alkyl) have been thoroughly studied during the last decade. For *trans*,*cis*-$[Ru(X')(I)(CO)_2$(α-diimine)], the lowest optically accessible excited state has an XLCT character, but MLCT for X = Cl. Dependent on the alkyl ligand, the XLCT excited state interacts

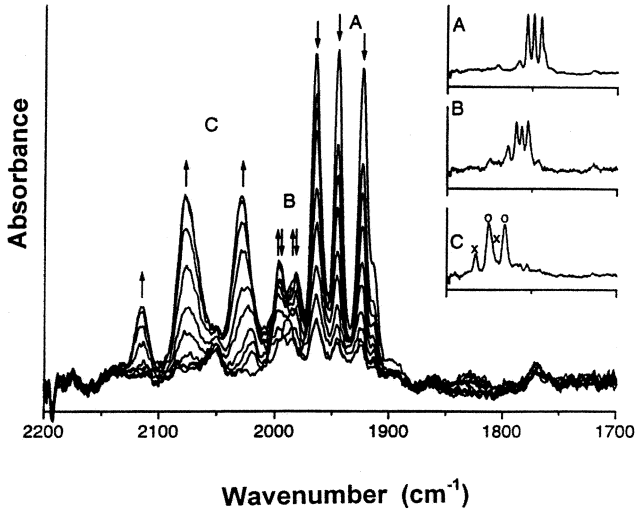

Fig. 3. IR spectral changes recorded during in situ oxidation of the complex *trans*{$Ru(CO)_2Cp$}-$[Ru\{Ru(CO)_2Cp\}_2(CO)_2(i\text{Pr-DAB})]$ from Section 3.4, recorded in butyronitrile at 193 K. The insets are the parent complex (A), the corresponding radical cation (B) and the secondary oxidation products *trans*(PrCN)-$[Ru(PrCN)_2(CO)_2(i\text{Pr-DAB})]^{2+}$ and $[Ru(PrCN)(CO)_2(Cp)]^+$, indicated by symbols x and o, respectively (C).

with various reactive states whose presence determines the photoreactivity of the complexes. For example in the case of X′ = methyl, a CO-loss reaction occurs as a first step of the photoisomerization of *trans*,*cis*-$[Ru(Me)(I)(CO)_2(i\text{Pr-DAB})]$ into its *cis*,*cis*-isomer, or CO-substitution by a donor solvent. On the other hand for X′ = benzyl or isopropyl, the reactive excited state possesses σ(Ru–Bz)π*(*i*Pr-DAB) character and its population results in a homolytic cleavage of the Ru–alkyl bond and the formation of corresponding radicals [39].

The behavior of the complex *trans*,*cis*-$[Ru(Me)(I)(CO)_2(i\text{Pr-DAB})]$ (ν(CO) at 2027, 1960 cm^{-1} (MeCN, 293 K); 2024, 1957 cm^{-1} (THF, PrCN, 183 K)) upon (electro)chemical reduction was reported for the first time by tom Dieck et al. who observed formation of the dimer *trans*(Me)-$[Ru(Me)(CO)_2(i\text{Pr-DAB})]_2$ (ν(CO) at 1981, 1952, 1921 cm^{-1} (MeCN, 293 K); 1982, 1954, 1924 cm^{-1} (THF, 293 K)). Further reduction of the dimer led to the five-coordinate anion $[Ru(Me)(CO)_2(i\text{Pr-DAB})]^-$ that was isolated as its potassium salt. (The IR spectrum has been reported for a closely analogous complex $K[Ru(Me)(CO)_2\{(i\text{Pr})_2\text{CH-DAB}\}]$: ν(CO) at 1910, 1835, 1915 cm^{-1} (THF, 293 K); the last ν(CO) band arising from a $CO\cdots K^+$ interaction) [86]. Our extended cyclic voltammetric and IR spectroelectroelectrochemical investigations of the reduction pathway of *trans*,*cis*-$[Ru(Me)(I)(CO)_2(i\text{Pr-DAB})]$ (Scheme 6) have confirmed the formation of the dimer *trans*(Me)-$[Ru(Me)(CO)_2(i\text{Pr-DAB})]_2$ by one-electron reduction of the parent complex at room temperature (Fig. 4a and Fig. 5). No transient radical species was observed in the course of the electrolysis. Subsequent reduction converted the dimer into $[Ru(Me)(CO)_2(i\text{Pr-DAB})]^-$ (Fig. 6); its Bu_4N^+-salt exhibits two intense ν(CO) bands at 1913, 1832 cm^{-1} (MeCN, 293 K) and 1915, 1835 cm^{-1}(THF, 293 K) [61].

Variation of the alkyl and halide ligands does not essentially alter the reduction pathway at 293 K. The same dimeric and anionic products are formed during the reduction of the parent complex *trans*,*cis*-$[Ru(Me)(Cl)(CO)_2(i\text{Pr-DAB})]$ (ν(CO) at 2024, 1952 cm^{-1} (THF, 293 K)). Analogous reduction products were observed also for *trans*,*cis*-$[Ru(Et)(I)(CO)_2(i\text{Pr-DAB})]$ (ν(CO) at 2019, 1955 cm^{-1} (THF, 293 K)): the dimer *trans*(Et)-$[Ru(Et)(CO)_2(i\text{Pr-DAB})]$ (ν(CO) at 1981, 1951, 1922 cm^{-1} (THF, 293 K)) and the anion $[Ru(Et)(CO)_2(i\text{Pr-DAB})]^-$ (ν(CO) at 1914, 1835 cm^{-1} (THF, 293 K)).

At this point we stress that the reduction pathway of the complexes *trans*,*cis*-$[Ru(X)(X')(CO)_2(i\text{Pr-DAB})]$ (X = halide, X′ = alkyl) at room temperature differs from those of the complexes *trans*(I)-$[Ru(I)_2(CO)_2(i\text{Pr-DAB})]$ and *trans*,*cis*-$[Ru(Cl)(X')(CO)_2(i\text{Pr-DAB})]$ (X′ = $SnPh_3$, $PbPh_3$, described in Section 3.3. In the latter case (see Scheme 2) the initial cathodic process consumes two electrons, as the five-coordinate radical

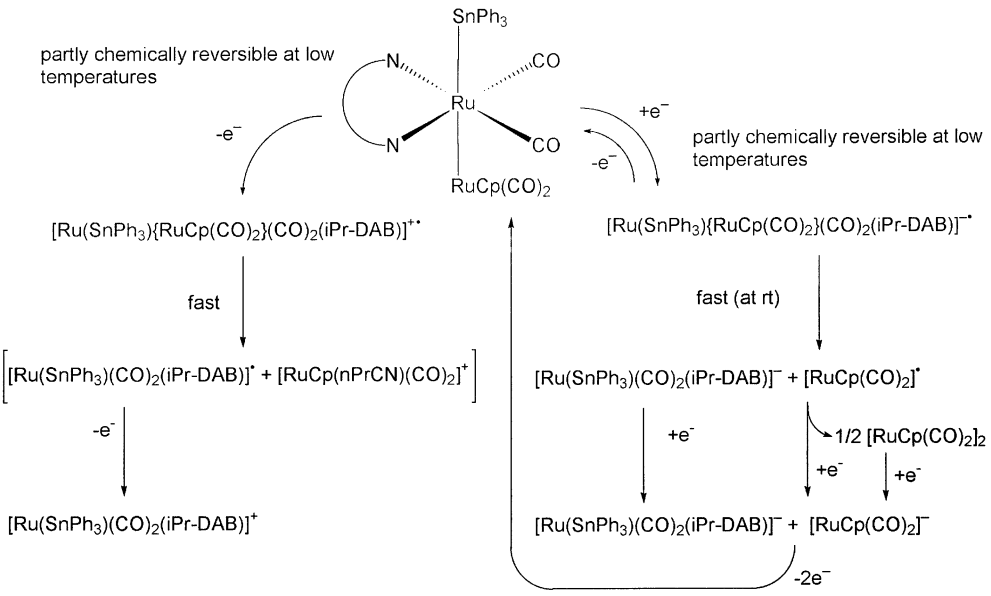

Scheme 4. Reduction and oxidation pathways of the complex *trans*,*cis*-[Ru(SnPh$_3$){Ru(CO)$_2$Cp}(CO)$_2$(*i*Pr-DAB)] described in Section 3.4.

transients [Ru(I)(CO)$_2$(*i*Pr-DAB)]$^\bullet$ and [Ru(X′)(CO)$_2$-(*i*Pr-DAB)]$^\bullet$ (X′ = SnPh$_3$, PbPh$_3$), formed by rapid halide loss from the corresponding one-electron reduced radical anions, are reduced *less negatively* than the parent complexes. Thus, the two-electron reduced five-coordinate anions [Ru(I)(CO)$_2$(*i*Pr-DAB)]$^-$ and [Ru(X′)(CO)$_2$(*i*Pr-DAB)]$^-$ (X′ = SnPh$_3$, PbPh$_3$) are formed at room temperature due to the ECE mechanism already at the reduction potential of the corresponding six-coordinate parent complex. Whereas the anions [Ru(I)(CO)$_2$(*i*Pr-DAB)]$^-$ lose another I$^-$ ligand and the Ru(0) products '[Ru(CO)$_2$(*i*Pr-DAB)]' become solvated or react with PR$_3$ or CO (but do not polymerize [76], differently from the analogous bpy-complexes in Section 3.1), the anions [Ru(X′)(CO)$_2$(*i*Pr-DAB)]$^-$ (X′ = SnPh$_3$, PbPh$_3$) react at room temperature with the yet non-reduced parent complexes, producing the dimers [Ru(X′)(CO)$_2$(*i*Pr-DAB)]$_2$ (Scheme 2). In contrast to this, the more negative electrode potential for the reverse oxidation of the anion [Ru(Me)(CO)$_2$(*i*Pr-DAB)]$^-$ (anodic peak D in Fig. 4a) compared to the reduction of parent *trans*,*cis*-[Ru(Me)(I)(CO)$_2$(*i*Pr-DAB)] (cathodic peak A in Fig. 4a), indicates that the five-coordinate radical transients [Ru(Me)(CO)$_2$(*i*Pr-DAB)]$^\bullet$ are reduced *more negatively* than the parent complex. The dimer [Ru(X′)(CO)$_2$(*i*Pr-DAB)]$_2$ (X′ = alkyl), observed at room temperature, is therefore formed by direct dimerization of [Ru(Me)(CO)$_2$(*i*Pr-DAB)]$^\bullet$ and not by the zero-electron coupling reaction between [Ru(X′)(CO)$_2$(*i*Pr-DAB)]$^-$ and *trans*,*cis*-

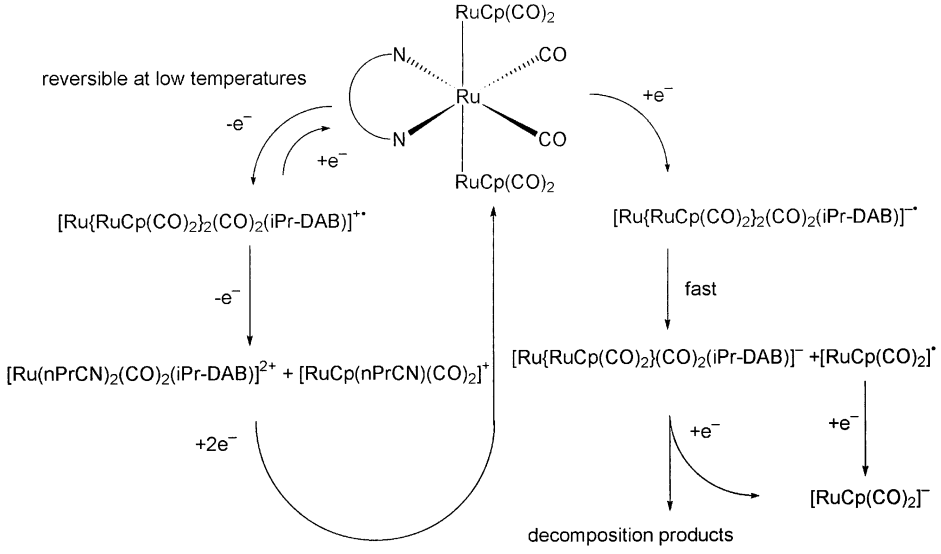

Scheme 5. Reduction and oxidation pathways of the complex *trans*{Ru(CO)$_2$Cp}-[Ru{Ru(CO)$_2$Cp}$_2$(CO)$_2$(*i*Pr-DAB)] described in Section 3.4.

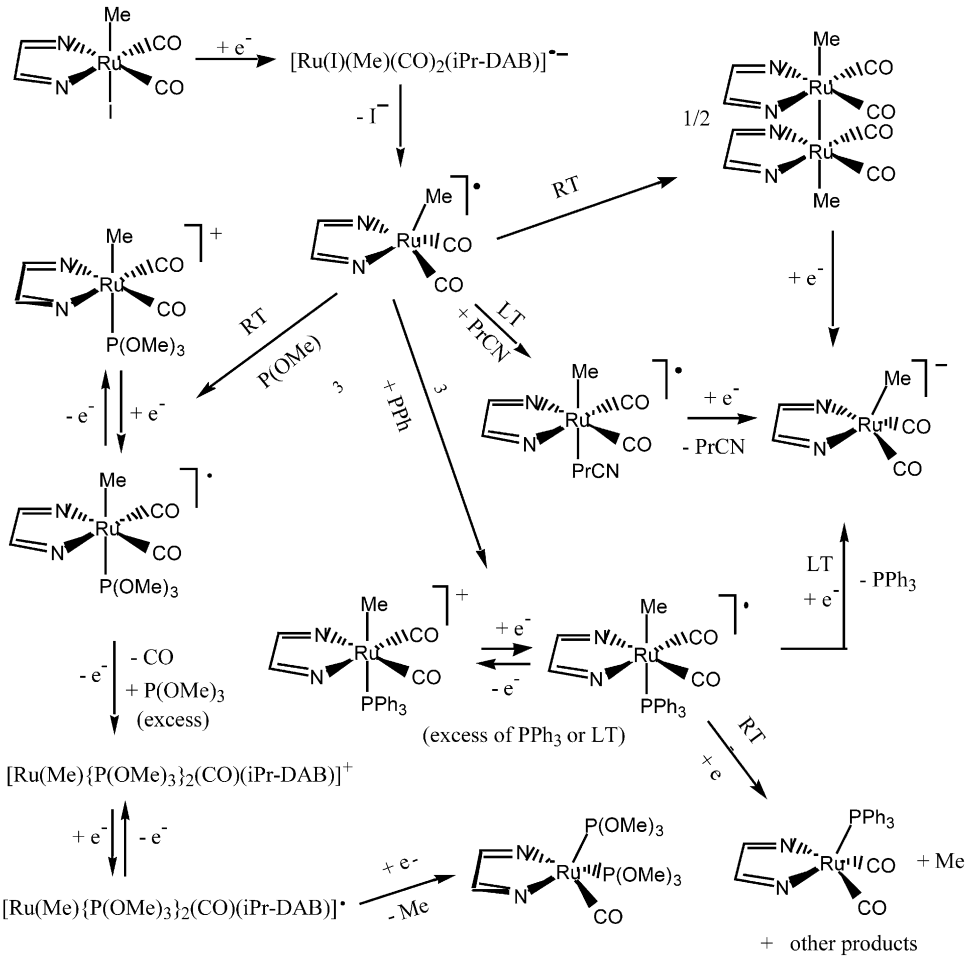

Scheme 6. Reduction pathway of the complex *trans*,*cis*-[Ru(Me)(I)(CO)$_2$(*i*Pr-DAB)] described in Section 3.5.

[Ru(X)(X′)(CO)$_2$(*i*Pr-DAB)] (X = halide, X′ = alkyl) that occurs e.g. for X′ = SnPh$_3$. The latter five-coordinate anions [Ru(X′)(CO)$_2$(*i*Pr-DAB)]$^-$ (X′ = alkyl) are only produced by the subsequent reduction of the dimers [Ru(X′)(CO)$_2$(*i*Pr-DAB)]$_2$ at more negative electrode potentials (cathodic peak B in Fig. 4a).

To obtain more evidence for the initial steps in the reduction pathway of the complexes and *trans*,*cis*-[Ru(X)(X′)(CO)$_2$(*i*Pr-DAB)] (X = halide, X′ = alkyl), we attempted to inhibit the dimerization reaction at low temperatures and to stabilize the radicals [Ru(Me)(CO)$_2$(*i*Pr-DAB)]$^\bullet$ or their more stable six-coordinate solvento forms [Ru(Sv)(Me)(CO)$_2$(*i*Pr-DAB)]$^\bullet$. The absence of the dimerization step was indeed proven by cyclic voltammetric (at 223 K) and IR spectroelectrochemical (at 183 K) experiments performed with *trans*,*cis*-[Ru(Me)(I)(CO)$_2$(*i*Pr-DAB)] in PrCN. The corresponding cyclic voltammogram (Fig. 4b) shows a new, reversible redox couple E that occurs less negatively then the reduction of the parent complex (cathodic peak A). The redox couple E has been assigned as *trans*,*cis*-[Ru(Me)(PrCN)(CO)$_2$(*i*Pr-DAB)]$^{+/\bullet}$. This means that the transient radical [Ru(Me)(CO)$_2$(*i*Pr-DAB)]$^\bullet$ did not dimerize or became instantaneously reduced in butyronitrile at 183 K but, instead, it converted into the six-coordinate radical *trans*,*cis*-[Ru(Me)(PrCN)(CO)$_2$(*i*Pr-DAB)]$^\bullet$. The formation of the latter complex was monitored in situ by IR spectroscopy (ν(CO) at 2000, 1924 cm^{-1} (PrCN, 183 K)), using a spectroelectrochemical cell (Fig. 7) [61]. In addition, the solvento radical *trans*,*cis*-[Ru(Me)(PrCN)(CO)$_2$(*i*Pr-DAB)]$^\bullet$ is also formed, together with [Mn(CO)$_5$]$^-$, upon one-electron reduction of the metal–metal bonded complex [(CO)$_5$Mn–Ru(Me)(CO)$_2$(*i*Pr-DAB)] [87] in PrCN at 183 K. This observation confirms the dissociation of the iodide ligand in the preceding case, upon the reduction of *trans*,*cis*-[Ru(Me)(I)(CO)$_2$(*i*Pr-DAB)].

In the presence of a large excess of PPh$_3$ (293 K), complex *trans*,*cis*-[Ru(Me)(I)(CO)$_2$(*i*Pr-DAB)] partly converted at the electrode potential of the onset of the one-electron reduction into the cationic species *trans*,*cis*-[Ru(Me)(PPh$_3$)(CO)$_2$(*i*Pr-DAB)]$^+$ (ν(CO) at 2046, 1976 cm^{-1} (THF, 293 K)) (Fig. 4c, cathodic peak A). This assignment has been confirmed by independent preparation of *trans*,*cis*-[Ru(Me)(PPh$_3$)(CO)$_2$(*i*Pr-

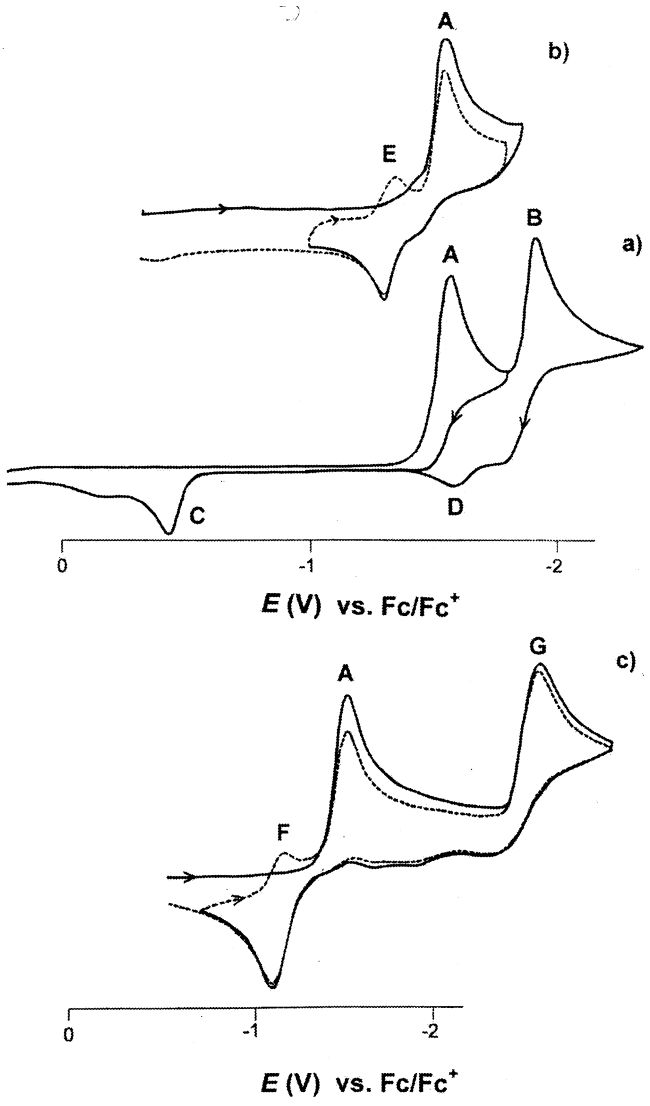

Fig. 4. (a) Cyclic voltammogram of the complex *trans*,*cis*-[Ru(Me)(I)$(CO)_2$(*i*Pr-DAB)] from Section 3.5 recorded in THF at 293 K and $v = 100$ mV s^{-1}. (A) Reduction of the parent complex; (B) reduction of the dimer *trans*(Me)-[Ru(Me)$(CO)_2$(*i*Pr-DAB)]$_2$; (C) oxidation of the dimer *trans*(Me)-[Ru(Me)$(CO)_2$(*i*Pr-DAB)]$_2$; (D) oxidation of the anion [Ru(Me)$(CO)_2$(*i*Pr-DAB)]$^-$. (b) Cyclic voltammogram of the complex *trans*,*cis*-[Ru(Me)(I)$(CO)_2$(*i*Pr-DAB)] from Section 3.5 recorded in PrCN at 223 K and $v = 100$ mV s^{-1}. (A) Reduction of the parent complex; (E) reversible redox couple *trans*,*cis*-[Ru(Me)(PrCN)$(CO)_2$(*i*Pr-DAB)]$^{+/\bullet}$. (c) Cyclic voltammogram of the complex *trans*,*cis*-[Ru(Me)(I)$(CO)_2$(*i*Pr-DAB)] from Section 3.5 recorded in THF containing an excess of PPh_3 at 293 K and $v = 100$ mV s^{-1}. (A) Reduction of the parent complex; (F) reversible redox couple *trans*,*cis*-[Ru(Me)$(PPh_3)(CO)_2$(*i*Pr-DAB)]$^{+/\bullet}$; (G) reduction of the radical *trans*,*cis*-[Ru(Me)$(PPh_3)(CO)_2$(*i*Pr-DAB)]$^\bullet$.

DAB)]$^+$ by stirring a solution of *trans*,*cis*-[Ru(Me)$(CF_3SO_3)(CO)_2$(*i*Pr-DAB)] in the presence of PPh_3. The fast substitution of I^- by PPh_3 is electrochemically induced (Eqs. (23) and (24)), since no such reaction occurred thermally even upon refluxing a solution of *trans*,*cis*-[Ru(Me)(I)$(CO)_2$(*i*Pr-DAB] and PPh_3 in THF for several hours. During continued

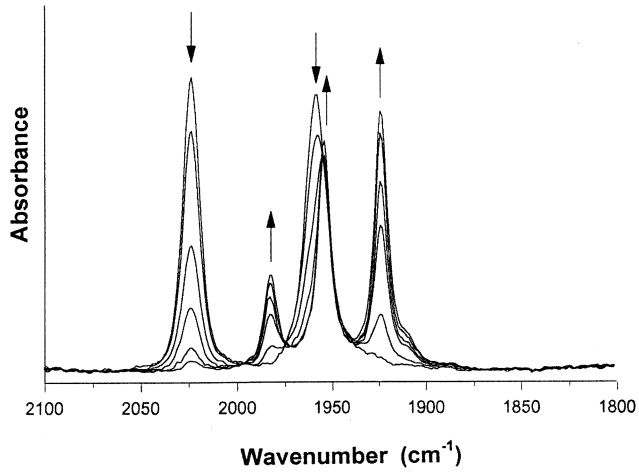

Fig. 5. IR spectral changes recorded during in situ reduction of the complex *trans*,*cis*-[Ru(Me)(I)$(CO)_2$(*i*Pr-DAB)] from Section 3.5 in THF at 293 K, producing the dimer *trans*(Me)-[Ru(Me)$(CO)_2$(*i*Pr-DAB)]$_2$.

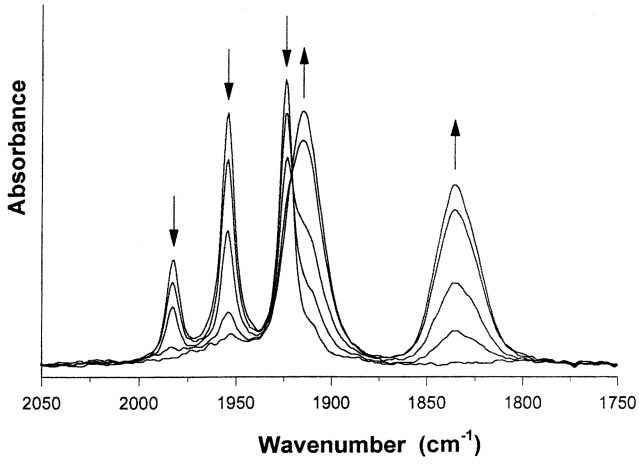

Fig. 6. IR spectral changes recorded during in situ reduction of the dimer *trans*(Me)-[Ru(Me)$(CO)_2$(*i*Pr-DAB)]$_2$ in THF at 293 K, producing the anion [Ru(Me)$(CO)_2$(*i*Pr-DAB)]$^-$.

reduction of *trans*,*cis*-[Ru(Me)(I)$(CO)_2$(*i*Pr-DAB], the more stable cationic complex *trans*,*cis*-[Ru(Me)(PPh_3)-$(CO)_2$(*i*Pr-DAB)]$^+$ was parallelly reversibly reduced into the corresponding radical (ν(CO) at 2004, 1937 cm^{-1} (THF, 293 K)), in agreement with the potential data in Table 2. This radical complex was also produced by irradiation of the dinuclear complex [$(CO)_5$Mn–Ru(Me)$(CO)_2$(*i*Pr-DAB)] in the presence of PPh_3 (EPR spectrum: $a(P) = 7.27$ mT, $2 \times a(N) = 0.77$ mT, $a(Ru) = 0.20$ mT, $a(H) < 0.13$ mT). Upon electrolysis of *trans*,*cis*-[Ru(Me)$(PPh_3)(CO)_2$(*i*Pr-DAB)]$^+$ at room temperature (Fig. 4c, cathodic peak F), the radical *trans*,*cis*-[Ru(Me)$(PPh_3)(CO)_2$(*i*Pr-DAB)]$^\bullet$ was the single reduction product only in the presence of a large excess of PPh_3 ($\gg$10:1). The subsequent reduction of *trans*,*cis*-[Ru(Me)$(PPh_3)(CO)_2$(*i*Pr-DAB)]$^\bullet$ (Fig. 4c, cathodic peak G) led to a mixture of carbonyl complexes, with [$Ru^0(PPh_3)(CO)_2$(*i*Pr-DAB)] (ν(CO) at

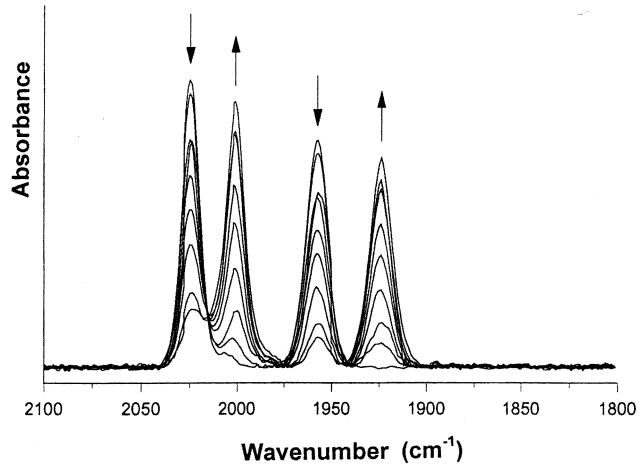

Fig. 7. IR spectral changes recorded during in situ reduction of the complex *trans*,*cis*-[Ru(Me)(I)(CO)$_2$(*i*Pr-DAB)] from Section 3.5 in PrCN at 183 K, producing the radical *trans*,*cis*-[Ru(Me)(PrCN)(CO)$_2$(*i*Pr-DAB)]$^\bullet$.

1970, 1966 cm^{-1} (THF, 293 K)) as a major component. The five-coordinate anion [Ru(Me)(CO)$_2$(*i*Pr-DAB)]$^-$ was formed alongside in low yield which increased with decreasing PPh_3 concentration. The reduction-induced dissociation of the methyl ligand instead of PPh_3 is a remarkable reaction, which was also investigated with $P(OMe)_3$ (see below). It could be inhibited at temperatures below 243 K, where the only two-electron reduced product formed was the anion [Ru(Me)(CO)$_2$(*i*Pr-DAB)]$^-$ (ν(CO) at 1913, 1832 cm^{-1} (PrCN, 183 K)).

$$\textit{trans},\textit{cis}\text{-[Ru(Me)(I)(CO)}_2\text{(}i\text{Pr-DAB]} + e^- \rightarrow \textit{trans},\textit{cis}\text{-[Ru(Me)(I)(CO)}_2\text{(}i\text{Pr-DAB]}^{\bullet -} \quad (23)$$

$$\textit{trans},\textit{cis}\text{-[Ru(Me)(I)(CO)}_2\text{(}i\text{Pr-DAB]}^{\bullet -} + PPh_3 \rightarrow \textit{trans},\textit{cis}\text{-[Ru(Me)(PPh}_3\text{)(CO)}_2\text{(}i\text{Pr-DAB]}^{\bullet} + I^- \quad (24)$$

A different reduction pathway of *trans*,*cis*-[Ru(Me)(I)(CO)$_2$(*i*Pr-DAB)] was observed in the presence of an excess of $P(OMe)_3$, which is a better π-acceptor with a smaller cone angle compared to PPh_3 (Scheme 6). Initially, the cationic complex *trans*,*cis*-[Ru(Me){P(OMe)$_3$}(CO)$_2$(*i*Pr-DAB)]$^+$ (ν(CO) at 2054, 1995 cm^{-1} (THF, 293 K)) was also formed as transient species at the onset of the one-electron reduction from an electrochemically induced reaction, like *trans*,*cis*-[Ru(Me)(PPh$_3$)(CO)$_2$(*i*Pr-DAB)]$^+$ (vide supra). Electrochemical reduction of the latter complex, however, does not produce a stable radical *trans*,*cis*-[Ru(Me){P(OMe)$_3$}(CO)$_2$(*i*Pr-DAB)]$^\bullet$ (Eqs. (25) and (26)). Instead, an electrode-catalyzed CO-substitution reaction takes place with the second $P(OMe)_3$ molecule (Eqs. (27) and (28)) to give the more negatively reducible [Ru(Me){P(OMe)$_3$}$_2$(CO)(*i*Pr-DAB)]$^+$ (ν(CO) at 1979 cm^{-1} (THF, 293 K)). Such a CO-substitution by PR_3 or $P(OR)_3$ in the singly reduced (radical) state is not uncommon; it has been for example reported for related Mn- and Re-tricarbonyl α-diimine [40,47] or *o*-semiquinone [88–90] complexes and for [M(CO)$_4$(α-diimine)] (M = Cr, Mo, W) [35,91]. In all these cases the phosphorus ligand occupies an axial position, as the reduction of the equatorial non-innocent chelated ligand weakens the metal–CO$_{ax}$ bond. For [Ru(Me){P(OMe)$_3$}$_2$(CO)(*i*Pr-DAB)]$^+$ the mutual position of the ligands has not been determined yet. Subsequent one-electron reduction of the latter monocarbonyl complex afforded smoothly the radical [Ru(Me){P(OMe)$_3$}$_2$(CO)(*i*Pr-DAB)]$^\bullet$ (ν(CO) at 1955 cm^{-1} (THF, 293 K)) that was further reduced to give a monocarbonyl product absorbing at 1927 cm^{-1}. This CO-stretching wavenumber agrees well with the value reported by van Dijk et al. for the formally d^8 Ru(0) complex [Ru{P(OMe)$_3$}$_2$(CO)(*i*Pr-DAB)] (Eq. (29)) [92]. This result again documents the remarkable labilization of the otherwise firmly bound methyl ligand, induced by the electrochemical reduction of the anionic *i*Pr-DAB ligand in the radical complexes in the presence of an excess of PR_3 or $P(OR)_3$.

$$\textit{trans},\textit{cis}\text{-[Ru(Me)(I)(CO)}_2\text{(}i\text{Pr-DAB]} + e^- \rightarrow \textit{trans},\textit{cis}\text{-[Ru(Me)(I)(CO)}_2\text{(}i\text{Pr-DAB]}^{\bullet -} \quad (25)$$

$$\textit{trans},\textit{cis}\text{-[Ru(Me)(I)(CO)}_2\text{(}i\text{Pr-DAB]}^{\bullet -} + P(OMe)_3 \rightarrow \textit{trans},\textit{cis}\text{-[Ru(Me)\{P(OMe)}_3\text{\}(CO)}_2\text{(}i\text{Pr-DAB]}^{\bullet} + I^- \quad (26)$$

$$\textit{trans},\textit{cis}\text{-[Ru(Me)\{P(OMe)}_3\text{\}(CO)}_2\text{(}i\text{Pr-DAB]}^{\bullet} + P(OMe)_3 \rightarrow [Ru(Me)\{P(OMe)_3\}_2(CO)(i\text{Pr-DAB}]^{\bullet} + CO \quad (27)$$

$$[Ru(Me)\{P(OMe)_3\}_2(CO)(i\text{Pr-DAB}]^{\bullet} \rightarrow [Ru(Me)\{P(OMe)_3\}_2(CO)(i\text{Pr-DAB})]^+ + e^- \quad (28)$$

$$[Ru(Me)\{P(OMe)_3\}_2(CO)(i\text{Pr-DAB}]^{\bullet} + e^- \rightarrow [Ru\{P(OMe)_3\}_2(CO)(i\text{Pr-DAB}] + Me^- \quad (29)$$

The reduction pathway of the complex *trans*,*cis*-[Ru(Me)(I)(CO)$_2$(bpy)] (ν(CO) at 2022, 1956 cm^{-1} (THF, 293 K)) is similar but not identical to that of *trans*,*cis*-[Ru(Me)(I)(CO)$_2$(*i*Pr-DAB)]. The major difference already involves the initial one-electron cathodic step at room temperature, which is chemically irreversible ($E_{p,c} = -1.99$ V vs. Fc/Fc$^+$) and causes dissociation of the iodide ligand (Fig. 8). Like for the *i*Pr-DAB ligand (vide supra), the resulting five-coordinate radicals [Ru(Me)(I)(CO)$_2$(bpy)]$^\bullet$ do not coordinate at room temperature a solvent molecule (THF or CH_3CN) but instantaneously dimerize. However, the expected metal–metal bonded dimer *trans*(Me)-[Ru(Me)(CO)$_2$(bpy)]$_2$ (ν(CO) at 1968, 1942, 1908 cm^{-1} (THF, 293 K)) is merely formed in a minor quantity, together with an air-stable major product denoted provisionally as '[Ru(Me)(CO)$_2$(bpy)]$_2$', possessing two intense ν(CO) bands at 1989 and 1916 cm^{-1} (THF, 293 K) (Fig. 9). Its oxidation at $E_{p,a} = -0.85$ V is irreversible (Fig. 8, anodic peak C) and recovers the parent complex, while

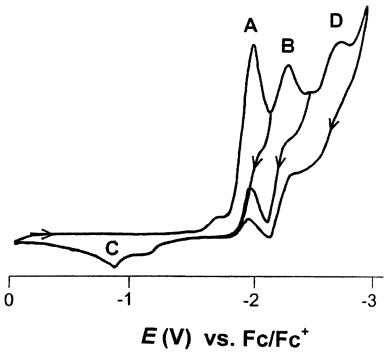

Fig. 8. Cyclic voltammogram of the complex *trans*,*cis*-[Ru(Me)(I)(CO)$_2$(bpy)] from Section 3.5 recorded in THF at 293 K and $v = 100$ mV s^{-1}. (A) Reduction of the parent complex; (B) reversible reduction of the yet little known complex '[Ru(Me)(CO)$_2$(bpy)]$_2$'; (C) oxidation of '[Ru(Me)(CO)$_2$(bpy)]$_2$' (assignment based on an independent cyclic voltammetric scan of '[Ru(Me)(CO)$_2$(bpy)]$_2$' under the same conditions; (D) cathodic process producing the anion [Ru(Me)(CO)$_2$(bpy)]$^-$.

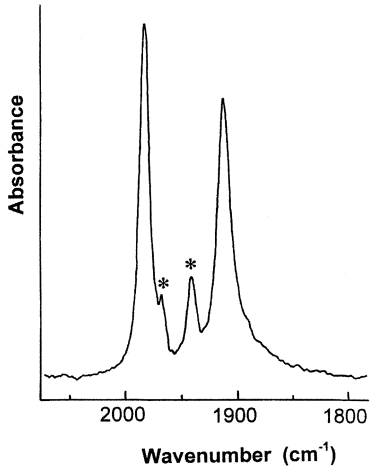

Fig. 9. IR spectrum recorded after the irreversible reduction of *trans*,*cis*-[Ru(Me)(I)(CO)$_2$(bpy)] from Section 3.5 in THF at 293 K. The two intense CO-stretching bands belong to '[Ru(Me)(CO)$_2$(bpy)]$_2$'. The small bands denoted with asterisk belong to the Ru–Ru bonded dimer *trans*(Me)-[Ru(Me)(CO)$_2$(bpy)]$_2$ (see Fig. 1).

its one-electron reduction at $E_{1/2} = -2.22$ V (vs. Fc/Fc$^+$) is reversible (Fig. 8, cathodic peak B) and affords a species absorbing at 1956 and 1876 cm^{-1}. Note, that these wavenumbers correspond neither to those of the insoluble polymer [Ru(CO)$_2$(bpy)]$_n$ (ν(CO) at 1966, 1908 cm^{-1}) [75] nor the five-coordinate anion [Ru(Me)(CO)$_2$(bpy)]$^-$ (ν(CO) at 1919, 1840 cm^{-1} (THF, 293 K)). The latter complex is the ultimate reduction product generated at $E_{p,c} = -2.72$ V (Fig. 8, cathodic peak D). This redox behavior points to a dinuclear structure of '[Ru(Me)(CO)$_2$(bpy)]$_2$'. Further studies are needed to resolve the structure and bonding properties of this complex.

The reduction of *trans*,*cis*-[Ru(Me)(I)(CO)$_2$(bpy)] becomes reversible at 183 K in PrCN on the time scale of CV ($v = 50$ mV s^{-1}). However, we did not succeed to detect the radical anion *trans*,*cis*-[Ru(Me)(I)(CO)$_2$(bpy)]$^{\bullet -}$ in the course of the corresponding IR spectroelectrochemical experiment. Instead, the IR spectra revealed the formation of '[Ru(Me)(CO)$_2$(bpy)]$_2$' (ν(CO) at 1974, 1897 cm^{-1}), together with a minor amount of the solvento radicals *trans*,*cis*-[Ru(Me)(PrCN)(CO)$_2$(bpy)]$^\bullet$ (ν(CO) at 1995, 1924 cm^{-1}). Subsequent reduction of both species directly produces the anion [Ru(Me)(CO)$_2$(bpy)]$^-$ (ν(CO) at 1914, 1841 cm^{-1} (THF, 293 K)). The UV–vis spectrum of the latter complex (Fig. 10) closely resembles those of [M(CO)$_3$(bpy)]$^-$ (M = Mn, Re), indicating the same bonding situation characterized by an extensively delocalized π-bonding within the Ru(bpy) metallacycle. A detailed comparison of these interesting five-coordinate complexes using (time-dependent) DFT calculations will be published in a forthcoming paper [49].

In the presence of PPh$_3$, the reduction pathway of *trans*,*cis*-[Ru(Me)(I)(CO)$_2$(bpy)] in THF at room temperature starts with the electrochemically induced conversion into the transitory cation *trans*,*cis*-[Ru(Me)(PPh$_3$)(CO)$_2$(bpy)]$^+$ (ν(CO) at 2039, 1983 cm^{-1}) that is further reduced into the stable radical *trans*,*cis*-[Ru(Me)(PPh$_3$)(CO)$_2$(bpy)]$^\bullet$ (ν(CO) at 2012, 1948 cm^{-1}). The following cathodic step gives rise to the instantaneous formation of the five-coordinate anion [Ru(Me)(CO)$_2$(bpy)]$^-$, together with a yet unassigned minor side-product absorbing at 1900 and 1851 cm^{-1}.

4. Concluding remarks

The above results show that as with the photophysical properties and photoreactivity, also the redox behavior of the title complexes *trans*,*cis*-[Ru(X)(X′)(CO)$_2$(α-diimine)] (X, X′ = halide, alkyl, donor solvent, metal carbonyl fragment like Mn(CO)$_5$, inorganometallic group like SnPh$_3$, phosphine) is strongly determined

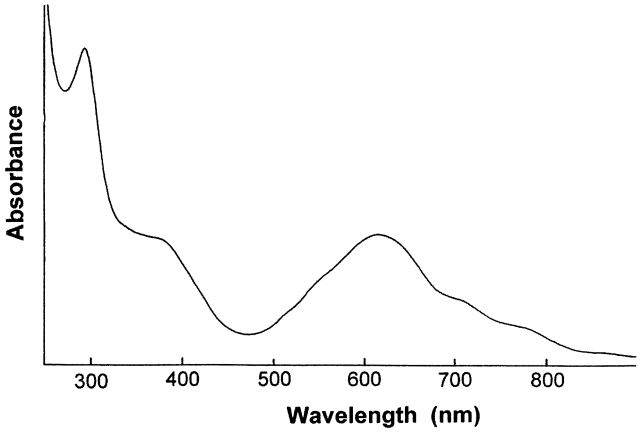

Fig. 10. UV–vis spectrum of the anion [Ru(Me)(CO)$_2$(bpy)]$^-$ in THF at 203 K.

by the nature of the axial ligands X and X′ and may conveniently be tuned to a great extent by choosing their proper combination. In this regard the title complexes resemble *fac*-[M(X)(CO)$_3$(α-diimine)]^n (M = Mn, Re; $n = 0, +1$), where the freedom of choice is however limited, with a few exceptions, to merely a single non-carbonyl ligand.

It has been noted that several reactions of *trans*,*cis*-[Ru(X)(X′)(CO)$_2$(α-diimine)] induced by photoexcitation and electrochemical electron transfer are identical, although the intimate mechanisms are usually different. As examples may serve CO-loss reactions induced by electrochemical oxidation and MLCT/XLCT photochemistry, or cleavage of Ru–X bonds (X = Me in the complex with X′ = $SnPh_3$, or metal carbonyl fragment such as $Mn(CO)_5$) from SBLCT excited states (homolytic Ru–X bond cleavage) and upon one-electron electrochemical reduction (usually producing X^- and a reactive, easily reducible 17e$^-$ radical ruthenium complex). A remarkable difference exists in this regard between the Ru–halide and Ru–alkyl bonds in mixed alkyl–halide complexes. Halide dissociation usually occurs upon electrochemical reduction but not upon MLCT/XLCT photoexcitation, characteristic for these complexes. In contrast to this, alkyl radicals are formed with a high quantum efficiency upon irradiation of mixed alkyl–halide complexes with a reactive SBLCT excited state lying at a lower energy than the optically accessible MLCT/XLCT excited state (e.g. X = Bz, *i*Pr), while the Ru–halide bond remains intact. Apparently, the σ- and π-donor halide ligand stabilizes the complex in the charge-transfer excited state with a partly oxidized metal center (CO dissociation is usually observed as a consequence). On the other hand, the Ru–alkyl bond cannot withstand transfer of electron density from the σ(Ru–alkyl) orbital towards the α-diimine ligand in the SBLCT excited state. In the one-electron reduced state, however, it is the weaker (less covalent) Ru–halide bond that dissociates due to a partial delocalization of the spin density from the equatorial [α-diimine]$^{\bullet -}$ ligand toward the axial X–Ru–X′ σ-system.

Comparison of the reviewed formally d^6 Ru(II) complexes *trans*,*cis*-[Ru(X)(X′)(CO)$_2$(α-diimine)] with the analogous Mn(I) and Re(I) compounds *fac*-[M(X)(CO)$_3$α-diimine)] allows one to analyze the main aspects of their reduction pathways, with a number of common points but also remarkable differences:

(a) The rhenium complexes generally form rather stable six-coordinate radicals/radical anions as products of the initial one-electron cathodic step. Also the two-electron reduced anionic complexes are commonly six-coordinate (e.g. for X = PR_3 or a donor solvent, in particular RCN). The nature (geometry) of the reduction products is mainly dependent on the electronic properties of the α-diimine ligand. If five-coordinate radicals are produced by X^- (= halide) dissociation, they preferably dimerize instead of being instantaneously further reduced to the corresponding anions.

(b) On the other hand, the manganese complexes tend to form preferably five-coordinate radical and anionic reduction products. The stabilizing influence of the strongly delocalized (CO)$_3$Mn(α-diimine) π-bonding is probably the main driving force for the dissociation of the axial two-electron donating ligand X independently of its electronic nature (alkyl, halide, phosphine, donor solvent, etc.). The π-delocalization becomes particularly extensive in the two-electron reduced anionic complexes. This property may explain the observed reduction of the five-coordinate radicals [Mn(CO)$_3$(α-diimine)]$^\bullet$ at a less negative electrode potential compared to the parent complex [Mn(X)(CO)$_3$(α-diimine)] (X = e.g. halide), introducing a two-electron ECE reduction pathway.

(c) The complexes *trans*,*cis*-[Ru(X)(X′)(CO)$_2$(α-diimine)] represent in many respects a transition between the Mn and Re complexes. For the same α-diimine ligand (e.g. *i*Pr-DAB), the one-electron reduced six-coordinate radicals/radical anions with the ruthenium center are in general substantially more stable than the tricarbonyl manganese complexes, but are much less stable than the rhenium-containing radicals. The stability of the inorganometallic radical anions with strongly delocalized axial X–Ru–X′ σ-bonds, described in Section 3.3, is extraordinary. The transient five-coordinate radicals [Ru(X′)(CO)$_2$(α-diimine)]$^\bullet$, when formed, may either directly dimerize (X′ = alkyl) or become first reduced to the corresponding anions (X′ = e.g. $SnPh_3$ or iodide). The actual pathway depends on the electronic properties of the formally anionic ligands X′ controlling the mutual position of the reduction potentials of the parent complex and the five-coordinate radical. We may conclude that the pronounced tendency of the complexes *trans*,*cis*-[Ru(X)(X′)(CO)$_2$(α-diimine)] to produce upon reduction the transient five-coordinate radicals [Ru(X′)(CO)$_2$(α-diimine)]$^\bullet$, further reducible to strongly π-delocalized anions [Ru(X′)(CO)$_2$(α-diimine)]$^-$, makes them closer related to the manganese rather then rhenium complexes *fac*-[M(X)(CO)$_3$α-diimine)]. Nevertheless, the stability of [Ru(X′)(CO)$_2$(α-diimine)]$^-$ (X′ = e.g. alkyl) is lower compared to the tricarbonyl anions [Mn(CO)$_3$(α-diimine)]$^-$, and neutral, formally d^8 Ru(0) complexes [Ru(X′)(CO)$_2$(α-diimine)] (X′ = e.g. CO, donor solvent, PR_3) are not uncommon as the ultimate reduction products.

(d) The two-electron reduction pathway of the complexes *trans*(Cl)-[Ru(Cl)$_2$(CO)$_2$(α-diimine)] with the fairly basic 2,2′-bipyridine or 1,10-phenathroline ligands is exceptional, resulting in facile gradual decoordination of the chloride ligands and formation of the polymeric chain [Ru(CO)$_2$(α-diimine)]$_n$. Having reduced the basicity of the α-diimine ligand by attachment of strongly

electron-withdrawing nitro groups, the polymerization process is inhibited on the dimer level. The same result is achieved by replacement of one chloride with a more firmly bound axial ligand, such as –C(O)OR.

Acknowledgements

Professor Dr. D.J. Stufkens and Dr. C.J. Kleverlaan (Universiteit van Amsterdam), Brenda D. Rossenaar (Akzo Nobel, Arnhem), Professor Dr. A. Vlček (Queen Mary and Westfield College, London), Professor Dr. C. Amatore and Dr. J.-N. Verpeaux (Ecole Normale Supérieure, Paris), Dr. A. Deronzier and S. Chardon-Noblat (Université J. Fourier, Grenoble) are acknowledged for their valuable contributions to the work reviewed in this article. We also wish to thank Professor Dr. A. Oskam (Universiteit van Amsterdam) for his great interest in the studies and many fruitful discussions. The Netherlands Foundation for Chemical Research (NWO) and COST D4 and D14 Actions are thanked for their financial support.

References

[1] K. Kalyanasundaram, Photochemistry of Polypyridine and Porphyrine Complexes, Academic Press, London, 1992.
[2] T.J. Meyer, Pure Appl. Chem. 58 (1986) 1193.
[3] E. Krausz, J. Ferguson, Progr. Inorg. Chem. 37 (1989) 293.
[4] R.J. Watts, J. Chem. Ed. 60 (1980) 834.
[5] D.M. Roundhill, Photochemistry and Photophysics of Metal Complexes, Plenum Press, New York, 1994.
[6] A. Juris, V. Balzani, F. Barigeletti, F. Campagna, P. Belser, A. von Zelewski, Coord. Chem. Rev. 84 (1988) 85.
[7] V. Balzani, A. Juris, Coord. Chem. Rev. 211 (2001) 97.
[8] V. Balzani, F. Scandola, Supramolecular Photochemistry, Horwood, Chichester, 1991.
[9] F. Scandola, M.T. Indelli, C. Chiorboli, C.A. Bignozzi, Top. Curr. Chem. 158 (1990) 73.
[10] V. Balzani, A. Juris, M. Venturi, S. Campagna, S. Serroni, Chem. Rev. 96 (1996) 759.
[11] D.J. Stufkens, Comments Inorg. Chem. 13 (1992) 359.
[12] M. Wrighton, D.L. Morse, J. Am. Chem. Soc. 96 (1974) 998.
[13] G.L. Geoffroy, M. Wrighton, Organometallic Photochemistry, Academic Press, New York, 1979.
[14] A. Juris, S. Campagna, I. Bidd, J.-M. Lehn, R. Ziessel, Inorg. Chem. 27 (1988) 4007.
[15] W. Kaim, H.E.A. Kramer, C. Vogler, J. Rieker, J. Organomet. Chem. 367 (1989) 107.
[16] P. Sullivan, J. Phys. Chem. 93 (1989) 24.
[17] L.A. Worl, R. Duesing, P. Chen, L. Della Ciana, T.J. Meyer, J. Chem. Soc. Dalton Trans. (1991) 849.
[18] P. Chen, T.D. Westmoreland, E. Danielson, K.S. Schanze, D. Anthon, P.E. Neveux, Jr., T.J. Meyer, Inorg. Chem. 26 (1987) 1116.
[19] K.S. Schanze, D.B. MacQueen, T.A. Perkins, L.A. Cabana, Coord. Chem. Rev. 122 (1993) 63.
[20] S. Campagna, G. Denti, S. Serroni, A. Juris, M. Venturi, V. Ricwevuto, V. Balzani, Chem. Eur. J. 1 (1995) 211.
[21] V. Balzani, S. Campagna, G. Denti, A. Juris, S. Serroni, M. Venturi, Acc. Chem. Res. 31 (1998) 26.
[22] R. Amadelli, R. Argazzi, C.A. Bignozzi, F. Scandola, J. Am. Chem. Soc. 112 (1990) 7099.
[23] M.K. Nazeeruddin, P. Liska, J. Moser, N. Vlachopoulos, M. Gratzel, Helv. Chim. Acta 73 (1990) 1788.
[24] B. Durham, J.V. Caspar, J.K. Nagle, T.J. Meyer, J. Am. Chem. Soc. 104 (1982) 4803.
[25] A. Vlček, Jr., Chemtracts: Inorg. Chem. 5 (1993) 1.
[26] K. Kalyanasundaram, J. Chem. Soc. Faraday Trans. 2 82 (1986) 2401.
[27] C. Kutal, M.A. Weber, G. Ferraudi, D. Geiger, Organometallics 4 (1985) 2161.
[28] C. Kutal, A.J. Corbin, G. Ferraudi, Organometallics 6 (1987) 553.
[29] J. Hawecker, J.-M. Lehn, R. Ziessel, Helv. Chim. Acta 69 (1986) 1990.
[30] O. Ishitani, M.W. George, T. Ibusuki, F.P.A. Johnson, K. Koike, K. Nozaki, C. Pac, J.J. Turner, J.R. Westwell, Inorg. Chem. 33 (1994) 4712.
[31] F.P.A. Johnson, M.W. George, F. Hartl, J.J. Turner, Organometallics 15 (1996) 3374 (and references 1–14 therein).
[32] H. Ishida, T. Terada, K. Tanaka, Inorg. Chem. 29 (1990) 905.
[33] J.R. Pugh, M.R.M. Bruce, B.P. Sullivan, T.J. Meyer, Inorg. Chem. 30 (1991) 86.
[34] H. Tanaka, H. Nagao, S.-M. Penk, K. Tanaka, Organometallics 11 (1992) 1450.
[35] D. Miholová, A.A. Vlček, J. Organomet. Chem. 279 (1985) 317.
[36] J. Víchová, F. Hartl, A. Vlček, Jr., J. Am. Chem. Soc. 114 (1992) 10903.
[37] A. Vlček, Jr., Coord. Chem. Rev. 200–202 (2000) 933.
[38] S. Chardon-Noblat, P. Da Costa, A. Deronzier, T. Mahabiersing, F. Hartl, Eur. J. Inorg. Chem., submitted for publication.
[39] D.J. Stufkens, A. Vlček, Jr., Coord. Chem. Rev. 177 (1998) 127.
[40] G.J. Stor, F. Hartl, J.W.M. van Outersterp, D.J. Stufkens, Organometallics 14 (1995) 1115.
[41] A. Klein, C. Vogler, W. Kaim, Organometallics 15 (1996) 236.
[42] F. Paolucci, M. Marcaccio, C. Paradisi, S. Roffia, C.A. Bignozzi, C. Amatore, J. Phys. Chem. Sect. B 102 (1998) 4759.
[43] J.W.M. van Outerstwerp, F. Hartl, D.J. Stufkens, Organometallics 14 (1995) 3303.
[44] B.P. Sullivan, M.R.M. Bruce, T.R. O'Toole, C.M. Bollinger, E. Megehee, H. Thorp, T.J. Meyer, in: W.M. Ayers (Ed.), Catalytic Activation of Carbon Dioxide, ACS Symp. Ser. 363, American Chemical Society, Washington DC, 1988, pp. 52–90.
[45] B.D. Rossenaar, F. Hartl, D.J. Stufkens, Inorg. Chem. 35 (1996) 6194.
[46] F. Hartl, R.P. Groenestein, T. Mahabiersing, Collect. Czech. Chem. Commun. 66 (2001) 52.
[47] B.D. Rossenaar, F. Hartl, D.J. Stufkens, C. Amatore, E. Maisonhaute, J.-N. Verpeaux, Organometallics 16 (1997) 4675.
[48] B.D. Rossenaar, PhD Thesis, University of Amsterdam, 1995.
[49] F. Hartl, P. Le Floch, P. Rosa, S. Záliš, manuscript in preparation.
[50] G.J. Stor, S.L. Morrison, D.J. Stufkens, A. Oskam, Organometallics 13 (1994) 2641.
[51] B.D. Rossenaar, A. Oskam, D.J. Stufkens, J. Fraanje, K. Goubitz, Inorg. Chim. Acta 247 (1996) 215.
[52] M.P. Aarnts, unpublished results.
[53] G.A. Carriedo, J. Gimeno, M. Laguna, V. Riera, J. Organomet. Chem. 219 (1981) 61.
[54] F.J.G. Alonso, A. Llamazares, V. Riera, M. Vivanco, S.G. Granda, M.R. Diaz, Organometallics 11 (1992) 2826.
[55] N.C. Brown, G.A. Carriedo, N.G. Connelly, F.J.G. Alonso, I.C. Quarmby, A.L. Rieger, P.H. Rieger, V. Riera, M. Vivanco, J. Chem. Soc. Dalton Trans. (1994) 3745.
[56] H. Bock, H. tom Dieck, Chem. Ber. 100 (1967) 228.
[57] H.A. Nieuwenhuis, D.J. Stufkens, A. Oskam, Inorg. Chem. 33 (1994) 3212.

[58] M.J.A. Kraakman, B. de Klerk-Engels, P.P.M. de Lange, K. Vrieze, W.J.J. Smeets, A.L. Spek, Organometallics 11 (1992) 3774.
[59] B. de Klerk-Engels, J.H. Groen, M.J.A. Kraakman, J.M. Ernsting, K. Vrieze, K. Goubitz, J. Fraanje, Organometallics 13 (1994) 3279.
[60] M. Krejcík, M. Daněk, F. Hartl, J. Electroanal. Chem. 317 (1991) 179.
[61] F. Hartl, H. Luyten, H.A. Nieuwenhuis, G.C. Schoemaker, Appl. Spectrosc. 48 (1994) 1522.
[62] M.-N. Collomb-Dunand-Sauthier, A. Deronzier, R. Ziessel, J. Organomet. Chem. 444 (1993) 191.
[63] E. Eskelinen, M. Haukka, T. Venäläinen, T.A. Pakkanen, M. Wasberg, S. Chardon-Noblat, A. Deronzier, Organometallics 19 (2000) 163.
[64] S. Luukkanen, M. Haukka, E. Eskelinen, T.A. Pakkanen, V. Lehtovuori, J. Kallioinen, P. Myllyperkiö, J. Korppi-Tommola, Phys. Chem. Chem. Phys. 3 (2001) 1992.
[65] H.A. Nieuwenhuis, D.J. Stufkens, A. Vlček, Jr., Inorg. Chem. 34 (1995) 3879.
[66] C.J. Kleverlaan, D.J. Stufkens, J. Photochem. Photobiol. A: Chem. 116 (1998) 109.
[67] C.J. Kleverlaan, F. Hartl, D.J. Stufkens, J. Photochem. Photobiol. A: Chem. 103 (1997) 231.
[68] A. Rosa, G. Ricciardi, E.J. Baerends, D.J. Stufkens, J. Phys. Chem. 100 (1996) 15346.
[69] A. Vlček Jr., I.R. Farrell, D.J. Liard, P. Matousek, M. Towrie, A.W. Parker, D.C. Grills, M.W. George, Dalton Trans., in press.
[70] M.-N. Collomb-Dunand-Sauthier, A. Deronzier, R. Ziessel, J. Electroanal. Chem. 350 (1993) 43.
[71] S. Chardon-Noblat, A. Deronzier, R. Ziessel, Collect. Czech. Chem. Commun. 66 (2001) 207.
[72] S. Chardon-Noblat, G.H. Cripps, A. Deronzier, J.S. Field, S. Gouws, R.J. Haines, F. Southway, Organometallics 20 (2001) 1668.
[73] S. Chardon-Noblat, A. Deronzier, D. Zsoldos, R. Ziessel, M. Haukka, T.A. Pakkanen, T. Venäläinen, J. Chem. Soc. Dalton Trans. (1996) 2581.
[74] S. Chardon-Noblat, P. Da Costa, A. Deronzier, M. Haukka, T.A. Pakkanen, R. Ziessel, J. Electroanal. Chem. 490 (2000) 62.
[75] C. Caix-Cecillon, S. Chardon-Noblat, A. Deronzier, M. Haukka, T.A. Pakkanen, R. Ziessel, D. Zsoldos, J. Electroanal. Chem. 466 (1999) 187.
[76] W. Rohde, H. tom Dieck, J. Organometal. Chem. 328 (1987) 209.
[77] M.P. Aarnts, F. Hartl, K. Peelen, D.J. Stufkens, C. Amatore, J.-N. Verpeaux, Organometallics 16 (1997) 4686.
[78] F. Hartl, M.P. Aarnts, K. Peelen, Collect. Czech. Chem. Commun. 61 (1996) 1342.
[79] L.H. Staal, L.H. Polm, R.W. Balk, G. van Koten, K. Vrieze, A.M.F. Brouwers, Inorg. Chem. 19 (1980) 3343.
[80] M.P. Aarnts, M.P. Wilms, K. Peelen, J. Fraanje, K. Goubitz, F. Hartl, D.J. Stufkens, E.J. Baerends, A. Vlček, Jr., Inorg. Chem. 35 (1996) 5468.
[81] M. Turki, Ch. Daniel, S. Zalis, A. Vlček, Jr., J. van Slageren, D.J. Stufkens, J. Am. Chem. Soc. 123 (2001) 11431.
[82] M.P. Aarnts, D.J. Stufkens, M.P. Wilms, E.J. Baerends, A. Vlček, Jr., I.P. Clark, M.W. George, J.J. Turner, Chem. Eur. J. 2 (1996) 1556.
[83] J. van Slageren, F. Hartl, D.J. Stufkens, D.M. Martino, H. van Willigen, Coord. Chem. Rev. 208 (2000) 309.
[84] M.P. Aarnts, D.J. Stufkens, A. Vlček, Jr., Inorg. Chim. Acta 266 (1997) 37.
[85] J. van Slageren, F. Hartl, D.J. Stufkens, Eur. J. Inorg. Chem. (2000) 847.
[86] H. tom Dieck, W. Rohde, U. Behrens, Z. Naturforsch. B 44 (1989) 158.
[87] (a) H.A. Nieuwenhuis, A. van Loon, M.A. Moraal, D.J. Stufkens, A. Oskam, K. Goubitt, Inorg. Chim Acta 232 (1995) 19;
(b) H.A. Nieuwenhuis, D.J. Stufkens, Inorg, Chem. 34 (1995) 3879.
[88] F. Hartl, D.J. Stufkens, A. Vlček, Jr., Inorg. Chem. 31 (1992) 1687.
[89] F. Hartl, A. Vlček, Jr., Inorg. Chem. 31 (1992) 2869.
[90] F. Hartl, A. Vlček, Jr., Inorg. Chem. 35 (1996) 1257.
[91] A. Vlček, Jr., F. Baumann, W. Kaim, F.W. Grevels, F. Hartl, J. Chem. Soc. Dalton Trans. (1998) 215.
[92] H.K. van Dijk, J.J. Kok, D.J. Stufkens, A. Oskam, J. Organomet. Chem. 362 (1989) 163.
[93] H. tom Dieck, W. Kollwitz, I. Kleinwächter, W. Rohde, L. Stamp, Transition Met. Chem. 11 (1986) 361.
[94] V.V. Pavlishchuk, A.W. Addison, Inorg. Chim. Acta 298 (2000) 97.